Development of *In Vitro* Diagnostic (IVD) Kits against Hepatitis A and E Infections

M.Sc. Thesis

By Omkar Raut



DEPARTMENT OF BIOSCIENCES AND BIOMEDICAL ENGINEERING INDIAN INSTITUTE OF TECHNOLOGY INDORE

May, 2025

Development of *In Vitro* Diagnostic (IVD) Kits against Hepatitis A and E Infections

A THESIS

Submitted in partial fulfillment of the requirements for the award of the degree

of Master of Science

by Omkar Raut



DEPARTMENT OF BIOSCIENCES AND BIOMEDICAL ENGINEERING INDIAN INSTITUTE OF TECHNOLOGY INDORE

May, 2025



INDIAN INSTITUTE OF TECHNOLOGY INDORE

CANDIDATE'S DECLARATION

I hereby certify that the work which is being presented in the thesis entitled "Development of In Vitro Diagnostic (IVD) Kits against Hepatitis A and E Infections" in the partial fulfillment of the requirements for the award of the degree of MASTER OF SCIENCE and submitted in the DEPARTMENT OF BIOSCIENCES AND BIOMEDICAL ENGINEERING, Indian Institute of Technology Indore, is an authentic record of my own work carried out during the time period June 2024 to May 2025 and year of joining the M.Sc. Program August 2023 to May 2025 under the supervision of Prof. Prashant Kodgire, Professor, BSBE, IIT Indore.

The matter presented in this thesis has not been submitted by me for the award of any other degree of this or any other institute.

> Signature of the student with date **Omkar Raut**

This is to certify that the above statement made by the candidate is correct to the best of my/our knowledge.

p.V. Wadgere Signature of the Supervisor

Prof. Prashant Kodgire

Omkar Raut has successfully given his/her M.Sc. Oral Examination held on 06-05-2025

Signature(s) of Supervisor(s) of MSc thesis
Date: 22/05/2025

ACKNOWLEDGEMENT

I want to thank everyone who has supported and guided me in this journey.

My supervisor, **Prof. Prashant Kodgire**, is one of those important people. Be it any doubts or troubles, he has never shown any disinterest, no matter how trivial, and has seen the problem through until we reached a meaningful solution. He has always corrected me when I was wrong and inspired me to do better every time. His determination and hardworking mentality have encouraged me to work hard. Again, thank you for allowing me to work under you and within your lab as your student.

I would also like to thank **Dr. Parimal Kar** (HOD, BSBE), my faculty advisor, **Prof. Ganti S. Murthy**, and all other teachers for teaching me the basics and imparting knowledge that will stay with me for the rest of my journey.

The lab of molecular immunology felt like my second family. Although I was not under anyone, everyone took me under their wing and guided me during my research. Mr. Brijeshwar Singh was one of those who guided me each time and taught me everything personally from scratch, just like a big brother would. Ms. Bindu Sai Vadaga and Ms. Surbhi Jaiswal were like my big sisters who supported me during my failures and encouraged me to improve. Mr. Saurav Sharma and Mr. Rahul Chaudhari were also there to help me and made doing research fun and lively. Ms. Krititka Malik also supported and helped me during my research. I would also like to thank the JRFs, Mr. Rishab Sai Batchu and Ms. Arundhuti Dey, who contributed to and helped me with this project. A special thanks to my friend Mr. Deveish Nigam, who was with me every time and helped me when I needed him most.

I want to thank AIIMS Bhopal for providing me with the serum samples and aiding me in my research. I would also like to thank ICMR for funding and initiating this project. The non-teaching staff helped me immensely, especially Mr. Arif Patel, Mr. Amit, Mr. Nilesh, and Mr. Gaurav Singh, by providing research materials and services.

I

Lastly, I would like to thank my parents, especially my **mother**, who worked hard to bring me up, and I wouldn't be here without her. She was always there for me and cheered me up in both good and bad situations—a big thanks to my friends and classmates for being with me and supporting me.

Thank you all for these wonderful two years!

- Omkar Raut

Abstract

Viral hepatitis, characterized by hepatic inflammation, is predominantly caused by hepatoviruses such as Hepatitis A virus (HAV) and Hepatitis E virus (HEV). This study aims to develop a rapid, in vitro diagnostic tool for detecting HAV and HEV infections using an antigen-based Lateral Flow Immunoassay (LFIA). The proposed diagnostic kit utilizes recombinant capsid proteins of HAV and HEV, which serve as specific antigens to capture anti-HAV/HEV IgM and IgG antibodies from patient serum samples. These antigens were produced by cloning the respective capsid protein genes into 'Escherichia coli' expression systems, followed by purification and validation through enzyme-linked immunosorbent assay (ELISA) to confirm antigenicity. Optimization of the ELISA protocol enabled clear serological differentiation between infected and uninfected human sera. Crossreactivity studies confirmed high specificity of the antigens, with negligible response against non-target hepatitis viruses. Statistical analysis further substantiated significant differences in optical density (O.D.) values between target-specific and non-specific interactions. Development of the LFIA device is ongoing, with current efforts focused on optimizing assay sensitivity, visual clarity, and consistency in differentiating positive and negative results.

Keywords: Hepatitis A, Hepatitis E, ELISA, LFIA, Diagnostics.



LIST OF PUBLICATIONS

From the thesis:

Development of *In Vitro* Diagnostic (IVD) Kits against Hepatitis A and E Infections (manuscript writing under preparation).



TABLE OF CONTENTS

LIST OF FIGURES	X
LIST OF TABLES X	Ι
ACRONYMS	
Chapter 1: Introduction	
1.1 Hepatitis	1
1.2 Hepatitis A	3
1.3 Hepatitis E	3
1.4 Enzyme-linked immunosorbent assay (ELISA)	1
1.5 Lateral flow immunoassays (LFIA)	5
1.6 Gold nanoparticles	0
Chapter 2: Objectives	3
Chapter 3: Materials and Methods	
3.1 Materials	5
3.2 Cloning of Ag1 gene of HEV and Ag2 gene of HAV16	6
3.3 Expression and purification of Ag1 (HEV) and Ag2 (HAV	7)
protein1	7
3.4 Dialysis of purified Ag1 of HEV and Ag2 of HAV protein17	7
3.5 Enzyme-linked immunosorbent (ELISA) assay to confirm	n
antigenicity of the Ag1 and Ag217	7
3.6 Conjugation of antigen with gold nanoparticles18	8
3.7 Synthesis of gold nanoparticles	3
3.8 Scanning Electron Microscopy	9
3.9 Conjugation of antigen to gold nanoparticles	9
3.10 Aggregation studies of gold nanoparticles and antigen20	0
3.11 Dipstick assembly20	0
3.12 Lateral immunoflow Kit development and assembly21	1

Chapter 4: Results and Discussion

APPENDIX-A	31
Chapter 5: Conclusion and Future Directions	
4.12 Lateral immunoflow Kit development and assembly	
4.11 Dipstick assembly results	
4.10 Aggregation studies using a blocking agent	
4.9 Optimization of conjugation	
4.8 SEM of synthesized AuNPs	39
4.7 Synthesis of AuNPs	36
4.6 Conjugation of AuNPs with protein	34
antigenicity of the Ag1 and Ag2	31
4.5 Enzyme-linked immunosorbent (ELISA) assay to confirm	ı
4.4 Dialysis of the purified protein	29
proteins	27
4.3 Expression and Purification of HEV Ag1 and HA	V Ag2
4.2 Colony and Plasmid PCR	25
(HAV) protein	23
4.1 Cloning, Expression, and purification of Ag1 (HEV) a	nd Ag2

LIST OF FIGURES

Figure 1.1. Schematic Representation of viral hepatitis
Figure 1.2. Schematic Representation of Indirect ELISA
Figure 1.3. Schematic Representation of various advantages of lateral flow
immunoassay
Figure 1.4. Schematic Representation of typical antigen-based LFIA10
Figure 1.5. Schematic Representation of AuNPs synthesis
Figure 1.6. Schematic Representation of antigen preparation
Figure 4.1.1. Agarose gels for plasmid preparation24
Figure 4.1.2. Insert preparation of HEV Ag124
Figure 4.1.3. Insert preparation for HAV Ag225
Figure 4.2.1 Colony and Plasmid PCR
Figure 4.2.2. Colony and Plasmid PCR results for HAV Ag226
Figure 4.3.1. Expression gel for HEV Ag127
Figure 4.3.2. Expression gel for HAV Ag2
Figure 4.3.3. Purification gel of HEV Ag1
Figure 4.3.4. Purification gel of HAV Ag2
Figure 4.4.1 Dialysis gel of HEV Ag130
Figure 4.4.2. Dialysis gel of HAV Ag230
Figure 4.5.1. ELISA graph showing the O.D. at 450 nm of HEV-infected
and healthy sera31
Figure 4.5.2. ELISA graph showing the O.D. at 450 nm of HAV-infected
and healthy sera
Figure 4.5.3. ELISA graph showing the O.D. at 450 nm of HEV-infected
healthy, HBV and HCV-infected sera32
Figure 4.5.4. ELISA graph showing the O.D. at 450 nm of HEV-infected
healthy, HAV, and dengue-infected sera
Figure 4.5.5. ELISA graph showing the O.D. at 450 nm of only serum
samples without antigen33
Figure 4.6.1. Spectral graph of conjugated AuNPs

Figure 4.6.2. Spectral graph showing the conjugation of AuNPs	in storage
buffer	35
Figure 4.6.3. Spectral graph showing the conjugation of AuNPs	with HAV
Ag2	35
Figure 4.7.1. Synthesis of AuNPs	36
Figure 4.7.2. Spectral graph showing the conjugation of AuNPs	with HAV
Ag2	37
Figure 4.7.3. Spectral graph showing the synthesiz	zed high
O.D	38
Figure 4.7.4. Spectral graph showing the synthesized high O.l	D. AuNPs
(diluted)	38
Figure 4.8.1. SEM analysis of synthesized AuNPs	39
Figure 4.9.1. Spectral graph showing the synthesized high O.l	D. AuNPs
conjugation optimization	40
Figure 4.10.1. Aggregation studies using a	blocking
agent	41
Figure 4.11.1. Dipstick assay with a blocking agent and without a	a blocking
agent conjugated antigen	42
Figure 4.11.2. Dipstick assay with a blocking agent conjugated an	ntigen and
HEV-infected sera	43
Figure 4.11.3. Dipstick assay with a blocking agent, conjugate	d antigen,
and healthy sera	
Figure 4.12.1. Development of LFIA kit	45

Acronyms

HEV- Hepatitis E Virus

HAV- Hepatitis A Virus

DAAS- Direct-acting antivirals

ELISA- Enzyme-Linked Immunosorbent Assay

LFIA- Lateral Flow Immunoassays

Ag- Antigen

Ab- Antibody

NC- Nitrocellulose

AuNPs- Gold Nanoparticles

O.D.- Optical Density

Taq- Thermus aquaticus

Pfu-Pyrococcus furiosus

Ni-NTA- Nickel nitriloacetic acid

SDS-PAGE- Sodium Dodecyl Sulphate Polyacrylamide Gel Electrophoresis

IPTG- Isopropyl β-D-thiogalactopyranoside

PCR- Polymerase Chain Reaction

HRP- Horse Radish Peroxidase

BSA- Bovine Serum Albumin

Chapter 1

Introduction

1.1 Hepatitis

Hepatitis is a term used to describe a condition of the liver where it succumbs to inflammation due to factors like viral infection, alcohol consumption, autoimmune diseases, etc. Viral Hepatitis is a liver inflammation caused by infection with a group of viruses. The most common family of viruses is the *hepatovirus* family. The family members include hepatitis types A, B, C, D, and E [1,2], each having different transmission methods, disease progressions, and potential health complications. Hepatitis can range from an acute to a chronic condition that may lead to severe liver damage, cirrhosis, or even fatal conditions like liver cancer [3,4]. Vaccination or some lifestyle changes can help prevent the occurrence of infection. However, some might require antiviral treatments to manage symptoms and initiate the self-healing process of the liver to prevent long-term damage. If not treated in time, it may lead to permanent liver damage and even death. Viral hepatitis is one of the significant causes of hepatitis cases in the world. Annually, around 300 million people are affected, which results in around 3.5 million deaths [5]. The fiercest types are B and C, of which B is the most notorious, affecting around 250 million people yearly [5]. Hepatitis A and E cause acute Hepatitis and can be cured in a few months. Both are transmitted through contaminated food and water (fecal-oral route) [6,7,8].

As mentioned earlier, hepatitis can be of two types, chronic and acute. Based on recent studies, it was found that almost all cases of acute viral hepatitis are caused either by hepatitis A or E, making them the epicenter of those infections. Even though not fatal, they can severely damage the liver, causing digestive problems, and sometimes a rare, life-threatening condition called "fulminant hepatitis". This can occur when a new acute infection occurs and requires urgent medical attention, since a person can go into sudden liver failure [9].

Symptoms of hepatitis are very vague at the early stages and might not give the impression of infection. The early symptoms include muscle and joint pain, fever, loss of appetite, abdominal pain, dark-coloured urine, itchy skin, etc. After a few days, these symptoms worsen, and additional symptoms like yellowing of the eyes and skin (jaundice), vomiting, and nausea appear. If not treated, they can lead to liver failure and even prove fatal in some cases [9].

Current treatments for viral hepatitis are limited. They are generally provided once the type of hepatitis is identified through medical diagnostics. Generally, type A virus is thrown out of the body by itself; rest and proper diet help. D and E are somewhat life-threatening and may require antiviral drugs and even a liver transplant in some cases.

For type B, antiviral medications like entecavir, tenofovir, lamivudine, and adefovir are used to suppress the virus and prevent liver damage. Direct-acting antivirals (DAA) treat hepatitis C [10]. These include sofosbuvir, ledipasvir, velpatasvir, elbasvir, grazoprevir, and glecaprevir [11]. Although liver transplantation may be needed in later stages of infection, when the liver is too severely damaged [12].

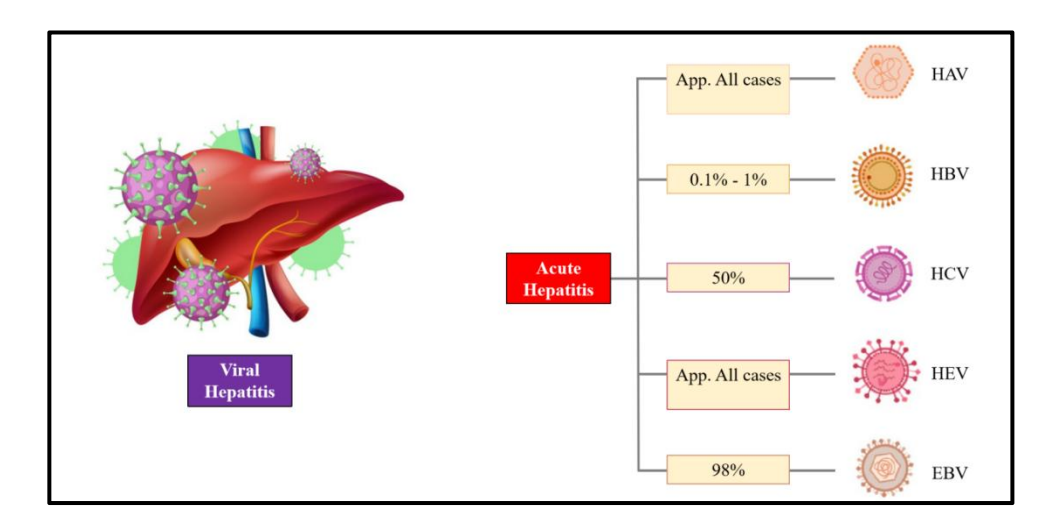


Figure 1.1. Schematic Representation of viral hepatitis along with the proportions of all types contributing to acute hepatitis.

1.2 Hepatitis A

Hepatitis A or *Hepatovirus* A is a virus species in *Picornavirales*, family *Picornaviridae*, genus *Hepatovirus* [13]. It is non-enveloped and has a positive strand of ssRNA as its genetic material [14]. Various human genotypes are numbered I–III, including six subtypes - IA, IB, IIA, IIB, IIIA, and IIIB [14]. It is mainly transmitted through the fecal-oral route, sometimes through blood, and uses vertebrates like humans as its replication hosts [15].

Hepatitis A diagnosis is done by detecting specific anti-HAV IgM antibodies formed within 1-2 weeks of infection and persist for a few weeks [16]. The capsid proteins of HAV are formed from 60 copies of four primary capsid proteins [17]. The highly immunodominant protein is Ag2, based on the high number of antibodies formed against its amino acids [18]. We aim to use genetic engineering to express the HAV Ag2 gene, one wild-type variant, and one codon-optimized variant in recombinant *E. coli* cells.

1.3 Hepatitis E

Hepatitis E or *Hepatovirus* E belongs to the family *Hepeviridae* [19]. Like HAV, it also has a positive strand of ssRNA as its genetic material. Its genome is divided into four major types - Genotypes 1,2,3,4 [20]. It encompasses various major open-reading frames that Ag1 encodes for three capsid proteins [21,22,23]. The transmission route is the same as HAV, through the fecal-oral route and blood [24]. For diagnosis, anti-HEV IgM antibodies developed in the body against HEV infection during the first weeks of infection are detected [25]. Out of the three classes described earlier, the truncated portion of Ag1 was the most immunodominant [26]. It was the protein of interest for purification to be used as an antigen in immunological tests.

1.4 Enzyme-linked immunosorbent assay (ELISA)

Early detection of these infections is essential to prevent further damage. Detection methods exist for all variants, primarily based on the serological reaction between antigen and antibody. The most reliable serological test used in immunodiagnostics is ELISA [27]. It detects the amount or presence of an antigen or an antibody in any sample (mostly body fluids) [27,28]. It is based on the principle of specific antigen and antibody (conjugated with a substrate) binding, where it utilizes an enzyme that catalyzes a color-changing reaction of the conjugated antibody's substrate, providing a detectable and measurable signal.

ELISA tests can be broadly classified into four main types: direct, indirect, sandwich, and competitive. These types are classified based on antigen-antibody binding and detection, leading to sensitivity, specificity, and application variations.

<u>Direct ELISA:</u> The target antigen is directly immobilized on the 96-well plate, and a labeled antibody (enzyme-conjugated) with affinity to the immobilized antigen is used to detect [27,28].

<u>Indirect ELISA:</u> The antigen is immobilized just like direct ELISA, but a primary antibody specific to the antigen is added first, and then a secondary antibody conjugated with an enzyme having affinity for the Fc portion of the primary antibody is used for detection [29] (Fig. 1.2).

<u>Sandwich ELISA:</u> Instead of an antigen, a primary antibody is coated onto the 96-well plate. The antigen from the sample is added, which binds to the coated antibody. After washing, the primary antibody is added, followed by a secondary antibody conjugated with an enzyme, or a secondary antibody is added directly [29].

Competitive ELISA: In competitive ELISA, inhibition of binding between the antigen and antibody occurs. The reference antigen is pre-coated on the 96-well plate. The sample containing an unknown antigen titer is incubated with a known titre of labeled antibody (conjugated to an enzyme), and then added to the wells. Both antigens compete for binding to the limited

quantity of labeled antibodies. The more antigen in the sample, the more it will bind to the labelled antibody and be washed off. This will result in a weaker output signal as the amount of labeled antibody bound to the plate is inversely proportional to the concentration of antigen in the sample [29].

ELISA is a reliable technique for detection purposes, but it takes time, substances, and expertise, which most people lack. Rapid antigen tests have been developed to confirm the positivity of a disease.

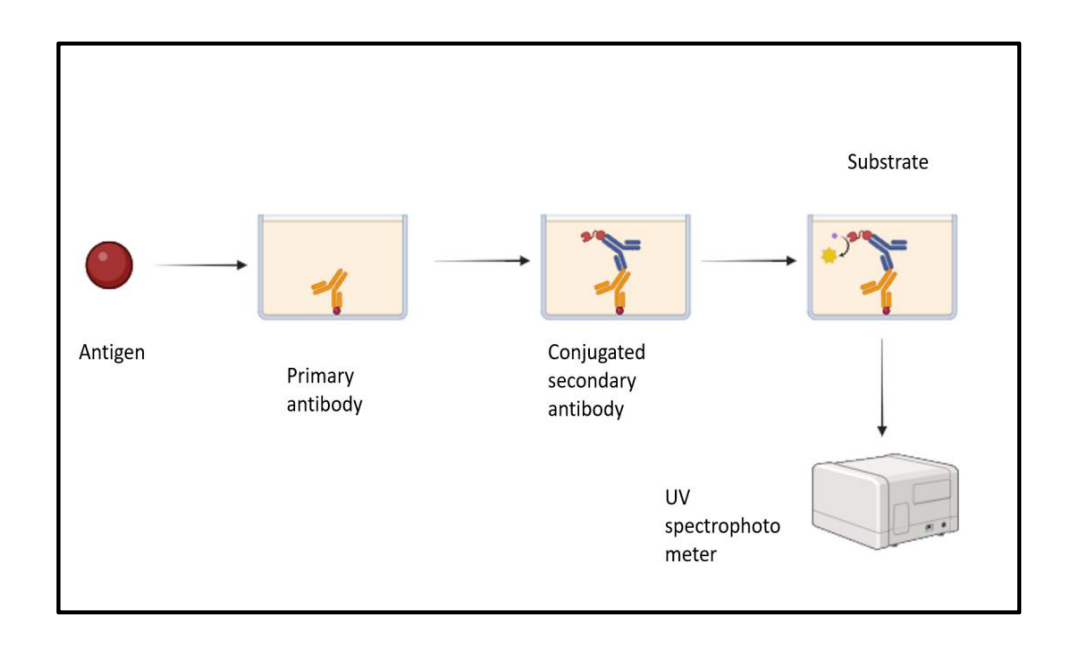


Figure 1.2. Schematic Representation of Indirect ELISA. Antigen is immobilised in the 96-well plate and then incubated with primary and enzyme-conjugated secondary antibody. The color formation following the addition of substrate is quantified using a plate reader.

1.5 Lateral flow immunoassays (LFIA)

LFIAs are the modern revolutionary medical diagnostics techniques that help rapidly detect molecules from a biological sample. LFIAs can be used for qualitative and semi-quantitative detection of various analytes such as antigens, antibodies, and haptens without needing professional skills and expensive instruments [30,31]. Biological samples may include hormones [32], pathogenic microorganisms [33,34], drugs [33], pesticides [35], biotoxins, and other targets [36,37]. LFIAs have a wider range of applications in point-of-care areas, such as hospitals, veterinary clinics, farms, dairies, labs, and other fields (Fig.1.3) [38,39].

LFIAs were first derived from the latex agglutination test established by Plotz and Singer [40]. The early application of LFIA was for determining human chorionic gonadotropin (hCG) in pregnant women's urine and serum/plasma in the late 1980s. These have gained attention due to their ease of use, affordability, and fast results. Later, LFIAs gained greater insight into detecting infections by quantifying the antigens and the antibodies from the patient's biological samples, significantly promoting the development of immune diagnostic technology [41].

Rapid tests are based on an immunological assay, LFIA (Lateral flow immunoassay). The basic principle is the same as ELISA. However, here, the antigen and the antibody conjugation yield a quicker response (within 2-3 min) and are highly sensitive to the concentration of antigen/antibody, but are not quantitative. It does not require expertise, is relatively cheaper, and is easier to set up than ELISA (Fig. 1.4) [42,43].

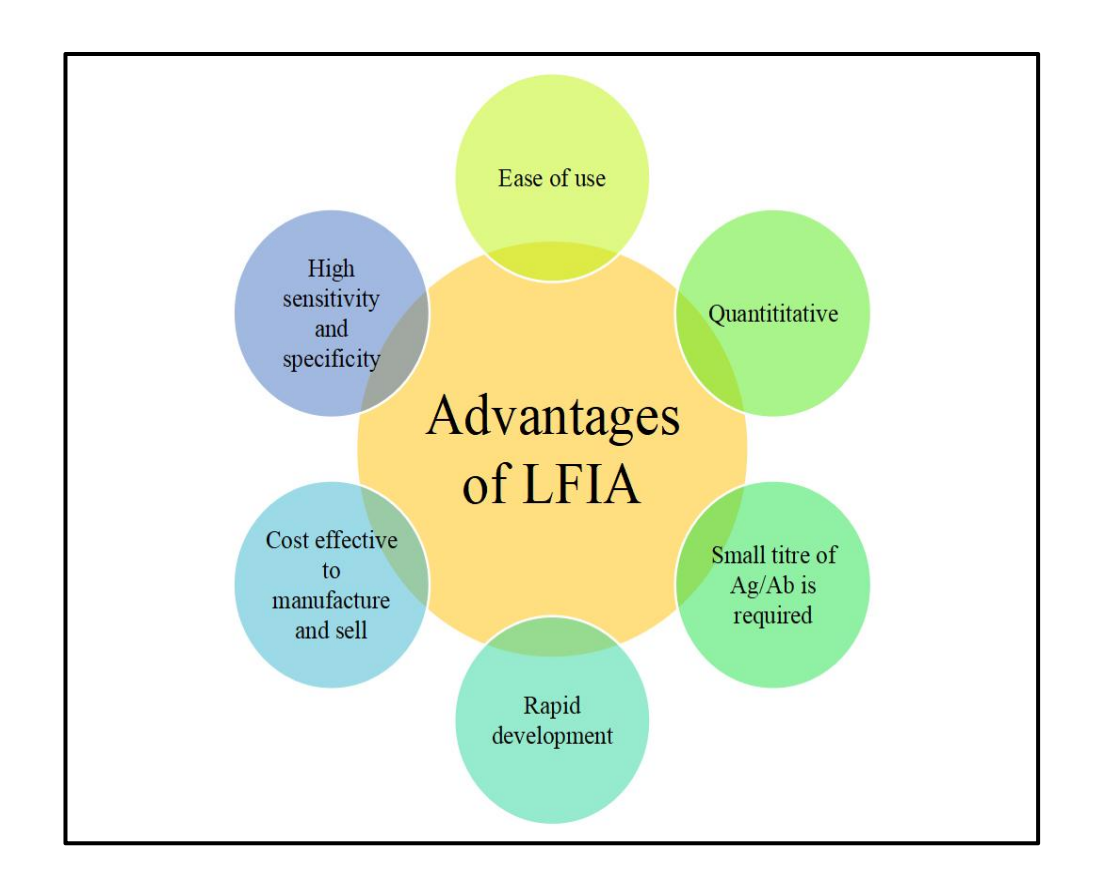


Figure 1.3. Schematic Representation of various advantages of lateral flow immunoassay.

Components of LFIA

A typical lateral flow immunoassay consists of four major components: a sample pad, a conjugate pad, an analytical pad, and an absorbent pad. Collectively, they formed the basis of immunoflow.

<u>Sample pad</u>: A dried sample pad can be used for loading. The sample may be blood, serum, urine, saliva, tears, etc.

<u>Conjugate pad</u>: The sample from the sample pad travels to the conjugate pad that contains conjugated detection labels such as gold nanoparticles. These gold nanoparticles can be conjugated to antigens or antibodies. These will play an important role in detecting the antigens and antibodies from the sample.

Analytical pad: This is the region where most of the magic happens. The analytical pad is mainly made up of nitrocellulose membrane or nylon

membrane. It has a higher affinity for proteins and hence can uptake antigens and antibodies. The serological reaction between the Ag/Ab and conjugated Ag/Ab results in aggregation and color formation. This indicates a positive reaction, referring to the presence of Ag/Ab in the sample. A pro test line with an Ag/Ab and an anti-human IgG antibody as a control is incubated to confirm the sample flow throughout the kit. This line should form a color every time, regardless of whether the sample is positive.

<u>Absorbent pad</u>: It absorbs the excess flow at the end to avoid spillage from the kit.

Two types of LFIA are practised in the scientific community: sandwich and competitive LFIA.

Sandwich LFIA:

The target analyte (protein, virus, hormone) must have at least two epitopes for binding to the antibody. The antigen will get sandwiched between two antibodies, one on the test strip and the other on the visualization antibody, mainly one conjugated with the gold nanoparticle.

Competitive LFIA:

This is used when the analyte is small (like drugs or toxins) and hence only has one epitope for binding to the antibody.

Here, the analyte in the sample competes with an immobilized analyte on the strip for a limited amount of labeled antibody.

The visual difference comes when both kits are developed. The sandwich one will have two colored lines, test and control, depicting positivity. Only one line at the control site represents the negativity of the analyte for which the test is conducted. In a competitive one, positivity is assessed by only one colored line at the control line site. If both lines are formed, the sample is negative for the given analyte. This occurs because the antigen/antibody competes with the labelled antigen/antibody and leaves no binding site for the Ag/Ab at the test line, leaving it blank.

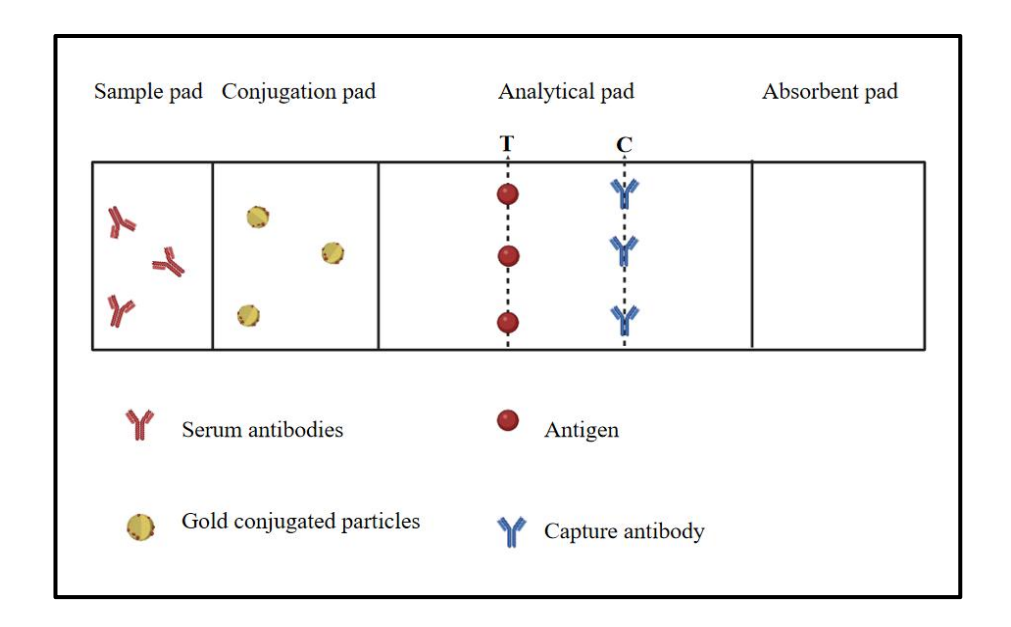


Figure 1.4. Schematic Representation of a typical antigen-based LFIA. The serum sample is loaded on the sample pad and flows from there to intereact with the gold conjugate to form a gold-Ag-Ab complex. This complex will interact with the antigen at the T (test line) and the capture antibody at the C (control line).

Antigen detection-based tests are more common than antibody ones as they can be used for the early detection of diseases. However, they are known to give a lot of false positives due to their lower sensitivity and potential crossreactivity with other pathogen proteins. Also, antibodies against specific antigens are expensive to make. The other option of antibody detection is the prime focus of this project, as neither A nor E is fatal, and early detection is needed. The purified antigen can capture anti-HV IgM antibodies formed within 4 days of infection and yield specific and accurate results.

1.6 Gold nanoparticles

Gold nanoparticles are one of the most heavily exploited nanomaterials in industries from 1-100 nm [44]. They are produced in various shapes, sizes, O.D., etc [45]. These properties determine their applications. Pharma, nanotechnology, healthcare, like kit development, gene therapy, immunosensing, drug delivery, tumor detection, etc., are some places where these particles are used extensively [46]. Gold nanoparticles for healthcare are prepared individually but are often conjugated to some biological agents for use. Antigen/antibody-conjugated AuNPs are primarily used in the healthcare industry, especially in developing kits [47]. Citrate-coated and pegylated AuNPs are used for the conjugation of antigen/antibody. Different methods have been employed for their chemical synthesis, including the Turkevich method, which is the most reliable and yields stable AuNPs. It uses a specific molar ratio of trisodium citrate to chloroauric acid for the synthesis of citrate-derived gold nanoparticles containing a negative charge that is stable at neutral pH (Fig. 1.5). Absorbance is a crucial aspect when it comes to determining the intensity of the band formed during kit development and should be higher than 4 (O.D.) for proper detection (Fig. 1.6) [48].

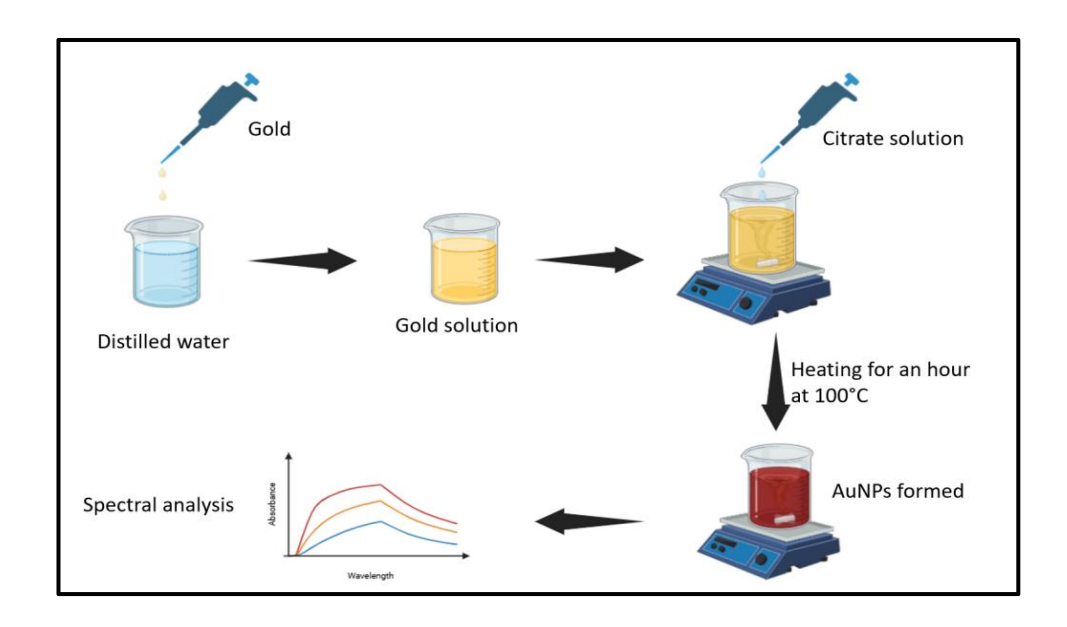


Figure 1.5. Schematic Representation of AuNPs synthesis. The gold solution is prepared in autoclaved distilled water and heated in a glass beaker at 100 °C. Sodium citrate is added in a ratio of 2:1 to gold and stirred and heated for 1 hour. Formation is considered when a colour change to red is observed, followed by confirmation analysis by spectra.

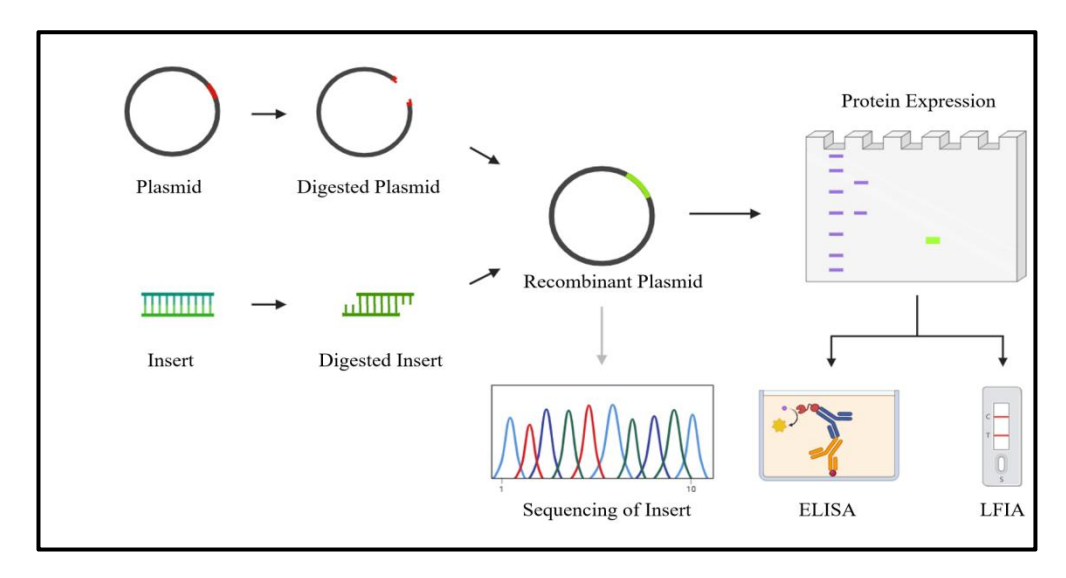


Figure 1.6. Schematic Representation of antigen preparation. The plasmid and insert were digested with restriction enzymes and ligated to form a recombinant plasmid, which was then transformed into an expression vector and sent for sequencing. The protein is expressed and purified. The purified protein is then used for ELISA and LFIA.

Chapter 2

Objectives

This study was based on three primary objectives designed and experimented with chronologically.

The three main objectives of the study were as follows:

- 1. Cloning, expression, and purification of structural proteins of HEV and HAV.
- 2. ELISA for detecting antigenicity of the purified protein of HAV and HEV.
- 3. Development of lateral flow-based rapid detection kit for HAV and HEV.

Chapter 3

Materials and Methods

3.1 Materials

HEV Ag1 gene and HAV Ag2 gene, primers specific for HEV Ag1 and HAV Ag2 genes, Taq polymerase, dNTPs, NdeI and XhoI restriction enzymes, Pfu DNA polymerase, T4 DNA ligase, plasmid extraction mini kit, plasmid gel purification kit, agarose gel electrophorectic apparatus, DH5α cells, pET43a vector, Ethidium bromide (EtBr). Luria Bertani broth, Luria Bertani agar, Bradford reagent, PMSF (Phenylmethanesulfonyl fluoride), Tris-Cl, Ni-NTA beads, Tween 20, Sodium hydrogen phosphate (Na₂HPO₄), Sodium dihydrogen phosphate (NaH₂PO₄), Sodium chloride (NaCl), Sodium dodecyl sulphate (SDS), Commassie brilliant blue G-250, β-mercaptoethanol, Acrylamide (C₃H₅NO), N, N'-Methylene bisacrylamide (MBAA), Tetramethyl ethylene diamine (TEMED), Ammonium sulphate ((NH₄)₂SO₄), dialysis membrane, Phosphate Buffer Saline (PBS), Urea (CH₄N₂O), Imidazole, SDS electrophoresis apparatus, staining and destaining solution. 96-well plate, Bovine serum albumin, skim milk, goat anti-human IgM secondary enzyme conjugated antibody, TMB (3,3',5,5'-Tetramethylbenzidine), sulphuric acid (H₂SO₄). Gold chloride (AuCl₃), Sodium trihydrate citrate, sample, conjugate, analytical, and absorbent pad.

3.2 Cloning of Ag1 gene of HEV and Ag2 gene of HAV

The complete Ag1 gene was obtained from our collaborators. It was used to amplify the truncated portion of the Ag1 gene, consisting of the immunodominant region. *Pfu* DNA polymerase amplified the template DNA using forward (HEV916F) and reverse (HEV917R) primers. The PCR cycles were programmed for an initial denaturation at 95 °C for 5 minutes, final denaturation at 92 °C for 30 seconds, annealing at 50 °C for 30 seconds, and extension at 72 °C for 50 seconds. The Final extension was

set for 10 minutes at 72 °C. The PCR products were confirmed on an agarose gel, purified, and subjected to double digestion using *NdeI* and *XhoI* restriction enzymes. The digested inserts were ligated with *NdeI* and *XhoI* double-digested pET43a, followed by transformation in DH5 α .

The HAV Ag2 gene was artificially synthesized and double-digested using NdeI and XhoI restriction enzymes. The plasmid was also double-digested using the same restriction enzymes. The obtained inserts and vectors were ligated, followed by transformation into DH5 α cells. The recombinant clones were screened by colony PCR, plasmid PCR, and final confirmation with DNA sequencing.

3.3 Expression and purification of Ag1 (HEV) and Ag2 (HAV) protein

The confirmed recombinant plasmids were transformed into E. coli (Rosetta) expression strains. The transformed colonies were inoculated in 6 mL of LB agar for 14 hours to express the desired protein. Secondary culture (400 mL) was inoculated by adding about 4 ml of primary culture for 3 hrs. O.D. of the secondary culture reached 0.8 after two and a half hours. About 0.5 mM of ITPG was added and incubated at 37 °C for four hrs. After 4 hours, the cells were subjected to lysis. Solubilization buffer (8 M urea, 300 mM NaCl, and 50 mM Tris-base, pH 8.0), about 5 ml, was used to solubilize the obtained pellet. The solubilization was subjected to centrifugation at 12500 rpm for 25 minutes. The supernatant was stored at 4 °C for purification. Purification was done using a gravity-based Ni-NTA column. 5 ml of solubilized protein was added to the column and equilibrated at room temperature for 2 hrs. Different buffers containing 8 M urea, 300 mM NaCl, 50 mM Tris-base, pH 8.0, and varying concentrations of imidazole, 20, 50, 100, 250, 500 mM, were used. The eluted samples were collected and confirmed using an SDS-PAGE gel.

3.4 Dialysis of purified Ag1 of HEV and Ag2 of HAV protein

Dialysis was performed using a dialysis membrane with the purified protein. Dialysis of about 1 mL of protein was done after precipitation by ammonium sulphate (1 M for HEV and 2 M for HAV). This was incubated at room temperature for 2 hours, and the precipitate obtained was solubilized in 8 M urea. This final solubilized protein was used for dialysis against 1X PBS (phosphate buffer saline) (1L) for 12 hours. The dialyzed protein was further used for immunoassays after confirmation by SDS PAGE.

3.5 Enzyme-linked immunosorbent (ELISA) assay to confirm antigenicity of the Ag1 and Ag2

In ELISA, the antigen was coated onto the surface of a well of 96-well plates. The antigen is diluted in carbonated buffer (pH 9.6) for better binding to the well surface overnight at 4 °C. The antigen is added to the well at a concentration. After overnight incubation, the wells are washed with 1X PBS solution containing Tween-20 at least 3 times to remove unbound antigens. Blocking was done to block the uncoated surface of the well using a blocking solution. The blocking solution contained skim milk in 1X PBS containing Tween-20. The blocking solution was added to the wells and incubated at 37 °C for two and a half hours. Wells were again washed with 1X PBS solution containing Tween-20 at least 3 times. The positive and negative sera from AIIMS Bhopal were used for primary antibodies. These serums were diluted in a ratio of 1:1000 with the standard diluent. About 100 μL of the diluted solution was added to the wells and incubated at 37 °C for 1 hr.

Wells were later washed with 1X PBS solution containing Tween-20 at least 5 times to remove unbound antibodies. The specific anti-HEV/HAV IgM antibodies from a positive patient will, if present, recognize the antigenic protein and bind to it. HRP conjugated secondary Antibody, namely, Goat anti-human IgM antibody, was used. The secondary antibody will bind specifically to the anti-HEV IgM antibody bound to the antigen. The secondary antibody is conjugated with the enzyme HRP, which will produce color once the substrate, 3,3′,5,5′-Tetramethylbenzidine (TMB), is added. The Antibody dilution in the ratio 1:2000 was used, and diluted secondary antibody was added to each well. The secondary antibody is allowed to bind for 1 hr at 37 °C. The wells are again washed with 1X PBS solution containing Tween-20 at least 5 times to remove unbound antibodies. Substrate TMB was added to each well. The enzyme will reduce the substrate if the secondary is still present in the well, bound to the primary antibody. Substrate is added to each well and incubated at room temperature for 20 minutes. The reaction was stopped after 20 minutes by adding 50 μL of stop solution (2 M H₂SO₄). The O.D. is taken at 450 nm in a plate reader to determine positive and negative samples.

3.6 Conjugation of antigen with gold nanoparticles

Gold nanoparticles (AuNPs), OD1, 20 nm, were centrifuged at 14,000 rpm for 20 min. The supernatant was discarded, and the pellet was suspended in half the volume of 0.1X PBS buffer. Protein was added to the solution and incubated on the rotary motor for 30 minutes. The conjugation was confirmed by the spectral analysis of the conjugated AuNPs using a UV spectrophotometer in the 400-600nm range. The conjugated AuNPs were further stored at 4 °C.

3.7 Synthesis of gold nanoparticles

To generate high optical density gold nanoparticles, we sought to synthesize them using the Turkewich method. Turkewich is a chemical method for synthesizing gold nanoparticles that uses sodium citrate and chloroauric acid (HAuCl₄) in a specific molar ratio. Firstly, the gold solution was prepared by adding 0.25 mM of HAuCl₄ into 95 mL of

autoclaved distilled water in a clean flask. The solution was heated up to 100 °C, and 1 M of sodium citrate was added in a dropwise manner so that the ratio of HAuCl₄ to sodium citrate would be 1:2. The reaction was stirred using a magnetic stirrer for about an hour at 100 °C. The change in color from yellow to red indicated gold nanoparticle formation. Spectral analysis was done to confirm the formation of gold nanoparticles.

3.8 Scanning Electron Microscopy

Scanning Electron Microscopy (SEM) is done to observe and confirm the size and morphology of the synthesized gold nanoparticles. Gold nanoparticles can be formed in various sizes and shapes. DLS can help us determine the size range, but fails to pinpoint the exact size and even the shape of the nanoparticles. SEM uses electron beams to scan the particles' surface and helps us accurately observe the size and shape of the nanoparticles.

3.9 Conjugation of antigen to gold nanoparticles

The conjugation plays a vital role in developing better lines on the NC membrane. The ratio by which the antigen and the AUNPs are mixed affects the overall conjugation. A conjugation method was employed to study the effect of different antigen volumes, where the volume of AuNPs was kept the same, but the volume of the antigen was changed. The ratios used were 1:10, 2:10, and 3:10 for the antigen and AuNPs. Each study was performed in duplicate with a volume of 500 μ L and was subjected to spectral analysis. While performing conjugation, the constant problem of precipitation of conjugates in the solution hampered the flow of gold particles on the NC membrane. To tackle this obstacle, a blocking agent was added. For this study, about 5 mg of a blocking agent was added to 500 μ L of O.D. 10 AuNPs. Later, about 100 μ L of antigen (HEV) was added to maintain the ratio of 2:10. Spectral analysis was done, and the graph for the same was plotted.

3.10 Aggregation studies of gold nanoparticles and antigen

Due to aggregation between the antigen and the AuNPs, precipitation hampers the flow of conjugated AuNPs on the NC membrane. Blocking can be done to avoid this, so a blocking agent is used. A blocking agent is assumed to coat the extra charge off the AUNPs (i.e., the negative charge (imparted through citrate) and hence aggregation is prevented.

For this experiment, 3 MCTs containing 5 gm of a blocking agent in 400 μ L of AuNPs (O.D. 10), 5 gm of a blocking agent in 400 μ L of AuNPs (O.D. 10), and 100 μ L of antigen. A control was also kept with 400 μ L of AuNPs (O.D. 10) and 100 μ L of antigen. The observation was done after incubating for 10 minutes at RT. Aggregation was noted when precipitation was observed against a clear solution.

3.11 Dipstick assembly

Before kit development, a special assay is done to confirm and optimize a few parameters. The dipstick assay determines the optimal flow rate, serum, antigen, and gold conjugate concentration. For this assay, nitrocellulose membranes are cut out (0.5cm in width each) and loaded with different antigen concentrations ranging from 2, 4, 8, 12 μ L using a micropipette in the form of a dot. Furthermore, the serum volume is also optimized by adding different volumes of 1:100 dilutions ranging from 40-120 μ L. The antigen-loaded NC is added to the gold-conjugated and serum-containing solution to observe the flow and development.

3.12 Lateral immunoflow Kit development and assembly

The main objective of this research was to develop a rapid, affordable, easy-to-use antigen-based kit. As mentioned before, the kit comprises four different parts. Each part was processed differently before assembling the final kit. The following treatments were given individually to the components.

Sample pad: Pad in Tris buffer saline (TBS) (pH 7.5) plus 1% BSA, 0.1% Tween 20, and incubation for 30 min at RT, followed by drying and incubation at 37 °C for 1 hr.

Conjugate pad: Pad in Phosphate buffer (pH 7.4) plus 1% BSA plus 2% Sucrose plus 0.2% Tween 20 for 30 min at RT, followed by drying and incubation at 37 $^{\circ}$ C for 1 hr. Spraying of AuNPs on the conjugate pad (10 μ l/cm) and drying for 15 min at 37 $^{\circ}$ C

Attach to the plastic backing card and incubate at 37 °C for 15 min

Analytical pad - Nitrocellulose membrane, Control line, sprayed with Goat anti-human IgG / IgM(1- 2mg/mL) at a 1 μ L/cm rate. Test line, Ag (1-2 mg/mL) at a rate of 1 μ L/cm

Absorbent pad: Drying of the pad at 37 °C for 1 hr.

After the components were ready, they were assembled using sterile forceps in a plastic cassette designed for kit development. The tests were then carried out to determine whether the kit works.

Chapter 4

Results and Discussion

4.1 Cloning, Expression, and purification of Ag1 (HEV) and Ag2 (HAV) protein

The plasmid isolation was carried out and the gel analysis of the same showed bands at 7.7 kb near the ladder (Fig. 4.1.1). The isolated plasmid underwent sequential digestion with *NdeI* and with *XhoI* resulting in 2 bands at the end in the gel reporting the isolated empty vector with sticky ends, suitable for insert ligation (Fig. 4.1.1.). The insert was prepared by amplifying the desire truncated part of the gene from the whole gene of HEV-Ag1 using the gene specific primers resulted in generation of a fragment which was observed in the gel run above 750 bp of the ladder (Fig. 4.1.2), as the truncated gene was 720 bp long. For HAV, the bands were observed around 900 bp on the gel. The digestion using the restriction enzymes *NdeI* and *XhoI* of the amplified insert of HEV and HAV genes resulted in a fragment with overhangs specific for the empty vector double isolated earlier. Both were run on a gel for confirmation and later used for ligation reaction (Fig. 4.1.2 and Fig. 4.1.3).

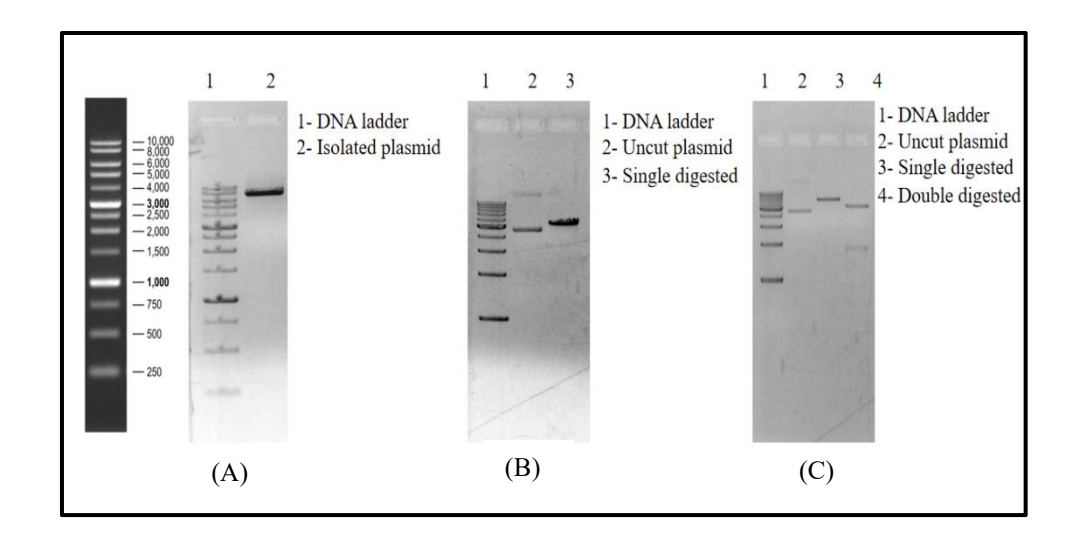


Figure 4.1.1. Agarose gels for plasmid preparation (A) pET42a (7.7 kb) plasmid was isolated using plasmid isolation kit (B) single digestion of pET42a using restriction enzyme *NdeI*, and (C) Double digestion of pET42a (5.5 kb) with restriction enzymes *NdeI* and with *XhoI* resulting in an empty plasmid and an insert.

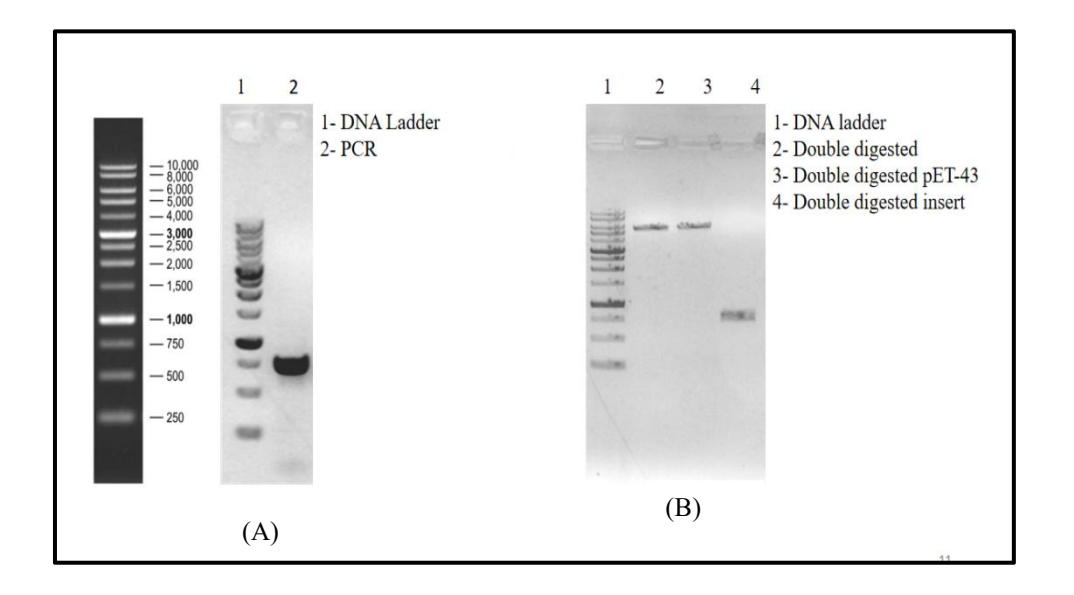


Figure 4.1.2. Insert preparation of HEV Ag1. (A) PCR product of HEV Ag1 (720 bp) above the 750 bp mark of the ladder, (B) Analytical gel of double-digested plasmid and insert.

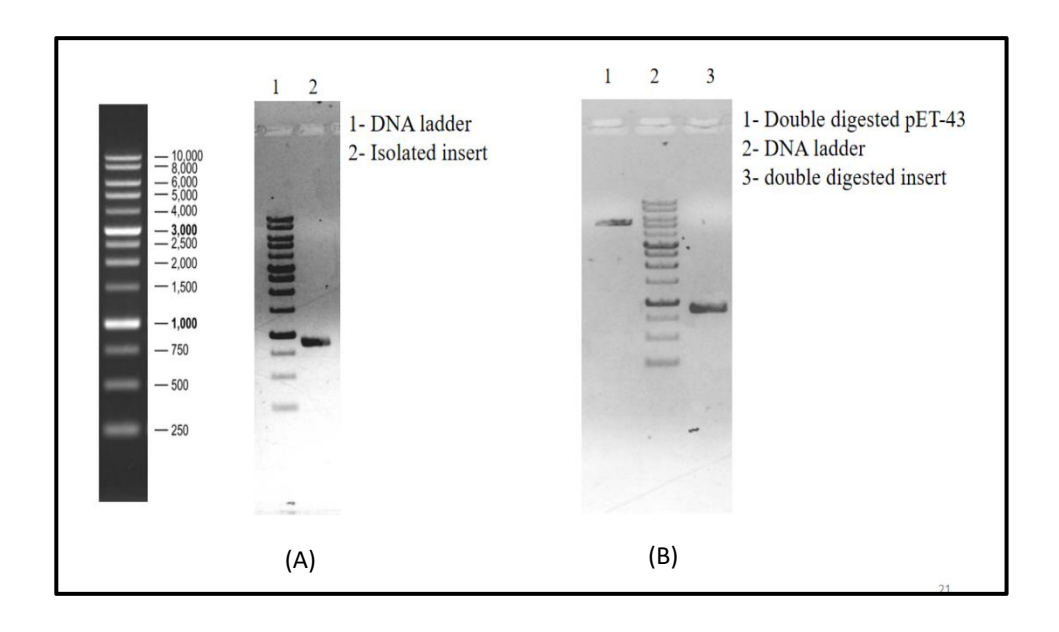


Figure 4.1.3. Insert preparation for HAV Ag2. (A) Insert (HAV Ag2) was isolated, showing a band around 900 bp. (B) Double digestion of the insert with the help of restriction enzymes NdeI and *Xho*I results in overhangs.

4.2 Colony and Plasmid PCR

Colony and plasmid PCR confirmed the successful ligation and cloning of the ligated recombinant plasmid in the cloning cells. Colony PCR represented bands of insert (720 bp) and the band in the positive control. Colonies representing clones 1, 2, 9,12 were selected for plasmid PCR (Fig. 4.2.1). Plasmid PCR of clones chosen 1, 2, 9, 12 revealed bands of 720 bp as expected when ran on an agarose gel (Fig. 4.2.1). For HAV, Colonies 8, 9, 10 showed positive colony PCR results with bands of 900 bp as observed on the gels. Confirmation of the exact clones from positive colonies was done by plasmid PCR using the same primers. It resulted in all clones showing bands of HAV Ag2, suggesting that the vector had taken up the insert (Fig. 4.2.2).

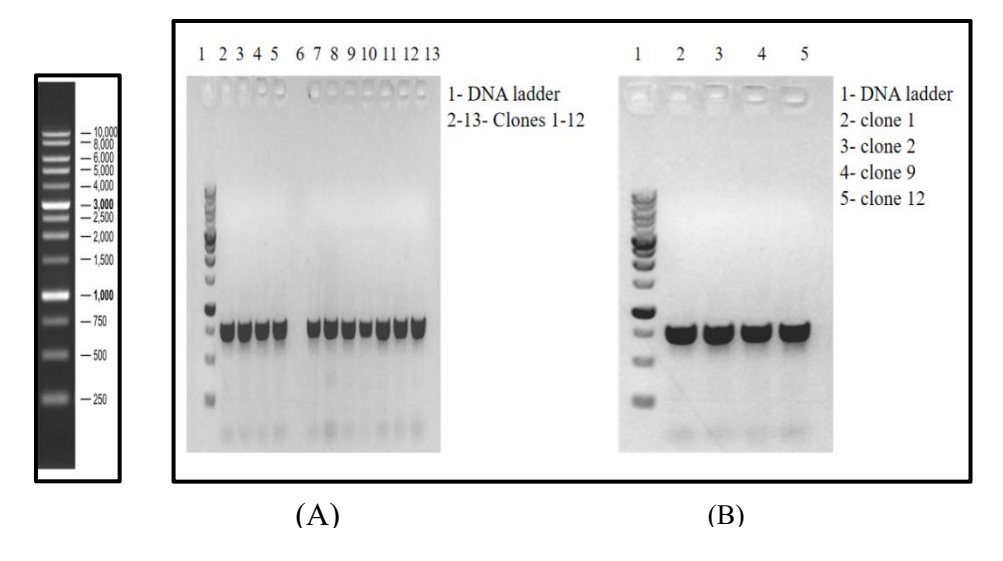


Figure 4.2.1. Colony and Plasmid PCR. (A) Colony PCR of the clones showed all clones had HEV Ag1 truncated gene, (B) Plasmid PCR of the selected clones from the colony PCR results (1, 2, 9, 12) using the same set of primers to confirm presence of HEV Ag1 truncated gene in the vector with bands of size 720 bp.

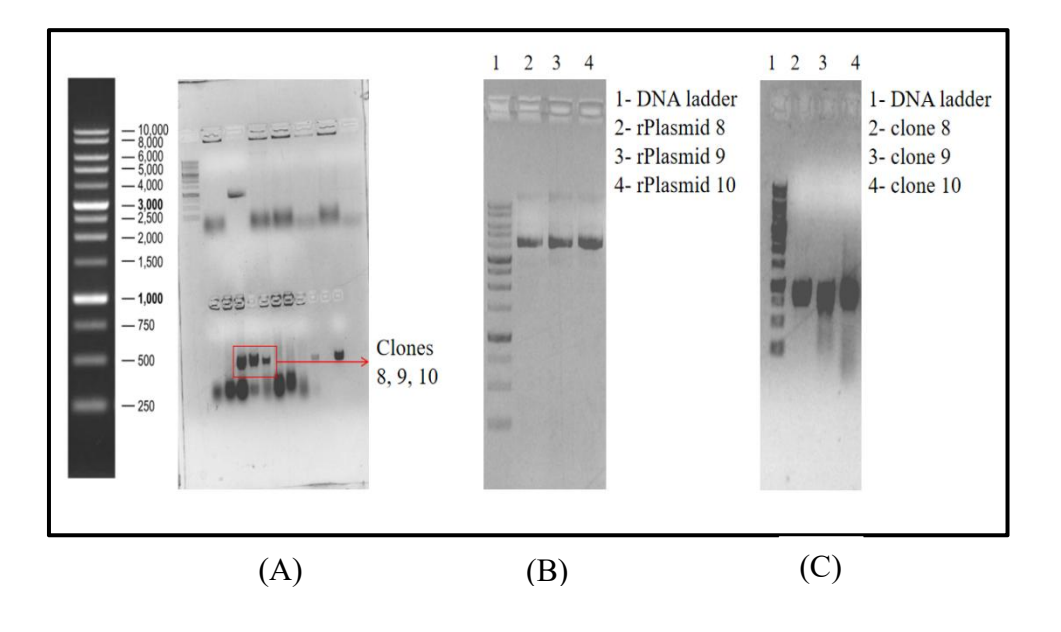


Figure 4.2.2. Colony and Plasmid PCR results for HAV Ag2. (A) Colony PCR showing positive inserts in clones 8, 9, 10 with a band size of 900 bp, (B) rPlasmid isolation from the clones using plasmid isolation kit, (C) Plasmid PCR of clones 8, 9, 10 confirms the insert presence in the vector.

4.3 Expression and Purification of HEV Ag1 and HAV Ag2 Proteins

The recombinant plasmid, verified by DNA sequencing, was transformed into *E. coli* Rosetta cells for HEV and HAV. The protein expression was carried out using 1 mM IPTG. An expression gel was run to check the expression of the proteins. A band was observed for HEV (Fig. 4.3.1) and HAV (Fig. 4.3.2) in the induced pellet fraction, suggesting the expression of both genes. The inclusion bodies of Ag1 and Ag2 were centrifuged after sonication and solubilized in 8 M urea buffer. Purification was done using a Ni-NTA column, wash, and elution buffers. All fractions were collected and run on a gel. Purified bands were observed for HEV in the fractions E1, E2, and E3 containing 100, 250, and 500 mM of imidazole (Fig. 4.3.3), and in fractions E2 and E3 containing 250 and 500 mM of imidazole for HAV (Fig. 4.3.4).

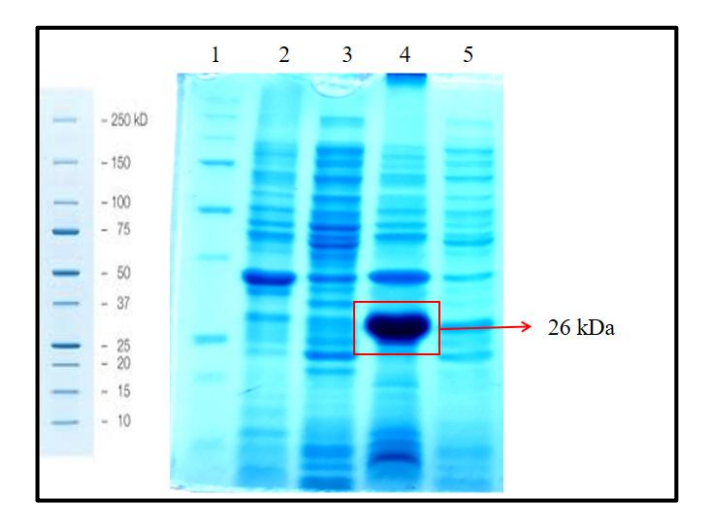


Figure 4.3.1. Expression gel for HEV Ag1. Lane 1 represents the protein marker, Lane 2 represents the uninduced pellet, Lane 3 represents the uninduced supernatant, Lane 4 represents the induced pellet, and Lane 5 represents the induced supernatant. A band is observed in the induced pellet fraction, confirming the successful production of HEV Ag1 protein.

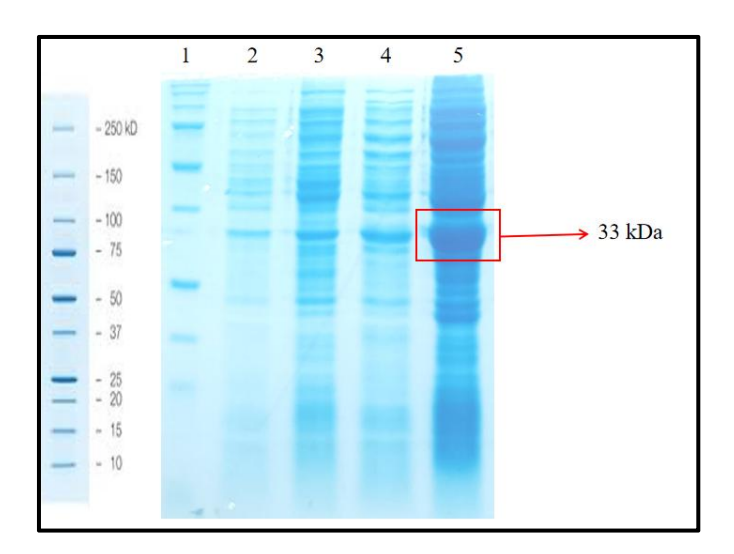


Figure 4.3.2. Expression gel for HAV VP3. Lane 1 represents the protein marker, Lane 2 represents the uninduced pellet, Lane 3 represents the uninduced supernatant, Lane 4 represents the induced pellet, and Lane 5 represents the induced supernatant. A band is observed in the induced pellet fraction, confirming the successful production of HAV Ag2 protein.

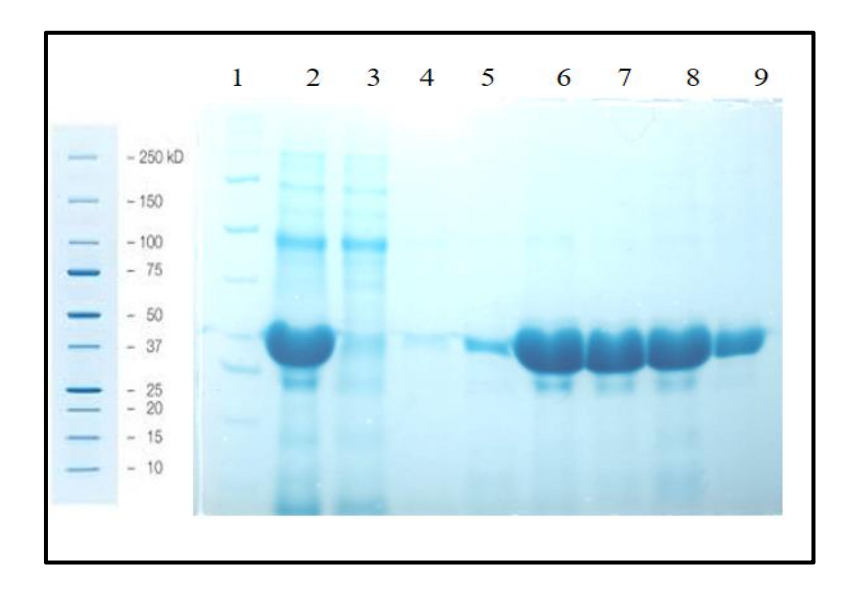


Figure 4.3.3. Purification gel of HEV Ag1. Lane 1 represents the unstained protein ladder, lane 2 represents input, Lane 3 represents flowthrough, Lane represents Wash buffer Lane 5 represents Wash 2 (20 mM Imidazole), Lane 6 represents Wash 3 (50 mM Imidazole), Lane 7 represents Elution 1 (100 mM Imidazole), Lane 8 represents Elution (250)mM Imidazole), Lane represents Elution 3 (500 mM Imidazole), Lane 10 represents Stripping buffer Shows that the protein has been eluted in 50, 100, 250, and 500 mM of imidazole.

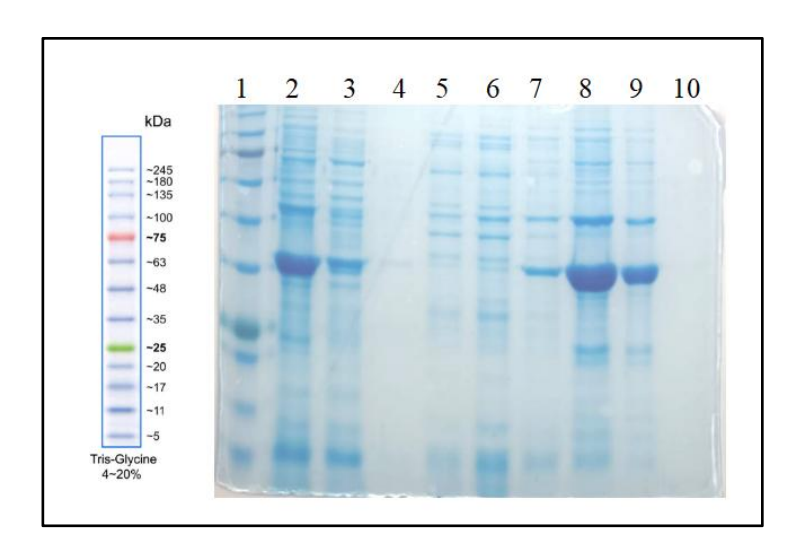


Figure 4.3.4. Purification gel of HAV Ag2. Lane 1 represents the unstained protein ladder, lane 2 represents input, Lane 3 represents flowthrough, Lane 4 represents Wash buffer Lane 5 represents Wash 2 (20 mM Imidazole), Lane 6 represents Wash 3 (50 mM Imidazole), Lane 7 represents Elution 1 (100 mM Imidazole), Lane 8 represents Elution 2 (250)mM Imidazole), Lane 9 represents Elution 3 (500 mM Imidazole), Lane 10 represents Stripping buffer Shows that the protein has been eluted in 50, 100, 250, and 500 mM of imidazole. Shows that the protein has been eluted in 100, 250, and 500 mM of imidazole.

4.4 Dialysis of the purified protein

The fractions containing the eluted purified protein were used for dialysis. Dialysis was done to change the buffer, make it suitable for further use, and increase stability. The fractions were first precipitated using ammonium sulphate (1 M for HEV and 2 M for HAV). A precipitate was immediately formed after the addition of ammonium sulphate. Centrifugation was done, and the precipitate obtained was then dissolved in 8 M urea. Dialysis was performed, and the resulting solution was run on an SDS PAGE for confirmation. Bands were observed in the respective lanes of HEV and HAV, suggesting that dialysis has occurred successfully (Fig. 4.4.1 and Fig. 4.4.2). Bands here were more purified because some unwanted proteins remained in the supernatant after the addition of ammonium sulphate. A few were lost in the process of dialysis. The dialyzed proteins were used for further immunoassays.

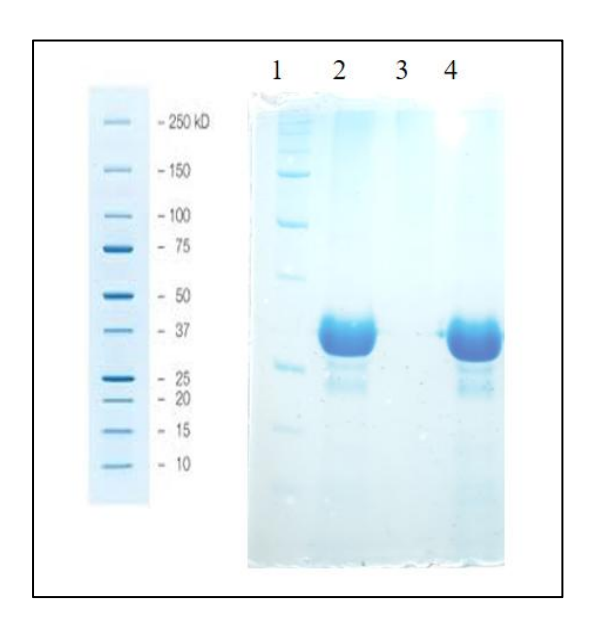


Figure 4.4.1. Dialysis gel of HEV Ag1. Lane 1 represents the protein marker, Lane 2 represents input, Lane 3 represents flowthrough, Lane 4 represents final dialyzed protein, and the band in Lane 4 represents the final dialyzed protein in PBS.

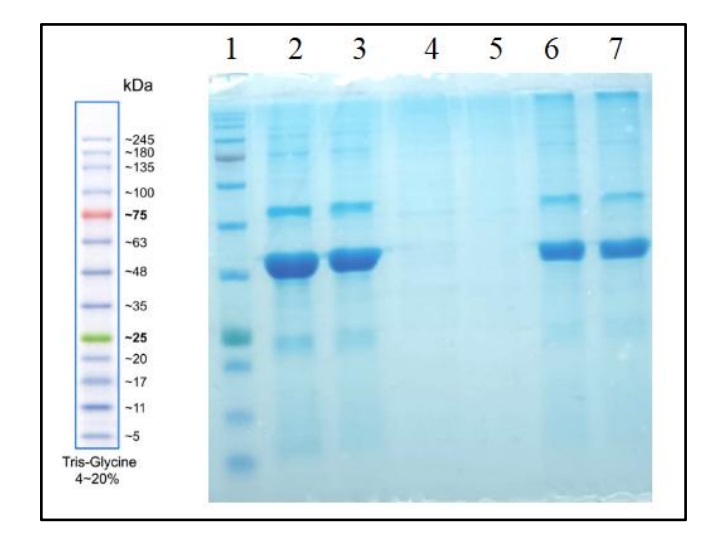


Figure 4.4.2. Dialysis gel of HAV Ag2. Lane 1 represents the protein marker, Lane 2 represents input, Lane 3 represents flowthrough, and Lane 4 represents the final dialyzed protein. The band in lane 4 represents the final dialyzed protein in PBS.

4.5 Enzyme-linked immunosorbent (ELISA) assay to confirm antigenicity of the Ag1 and Ag2

ELISA was done to check the antigenicity of the dialyzed pure proteins. ELISA results yielded a significant difference between positive and negative samples. At an antigen concentration of 100 ng/mL and serum dilution of 1:1000, the results obtained for HEV and HAV-infected samples were promising compared to those of healthy samples. Fig. shows that HEV and HAV samples have a significantly higher O.D. than the healthy samples at the end of the ELISA reaction. This suggests that the purified protein acts as an antigen for the anti-HEV and anti-HAV IgM antibodies (Fig. 4.5.1 and Fig. 4.5.2). crossreactivity assays with other viral serums of Hepatitis B virus, Hepatitis C virus, dengue, etc. resulted in the positive result as observed by higher O.D. in HEV and HAV respective samples than in other serum samples, suggesting that each protein has specificity for the corresponding anti-IgM antibodies and vice-versa (Fig. 4.5.3 and Fig. 4.5.4). ELISA against pure serum with no antigen (Fig. 4.5.5) was also done to check if any serum gave false positive results. The results verified that no antigen was present in the given serum samples.

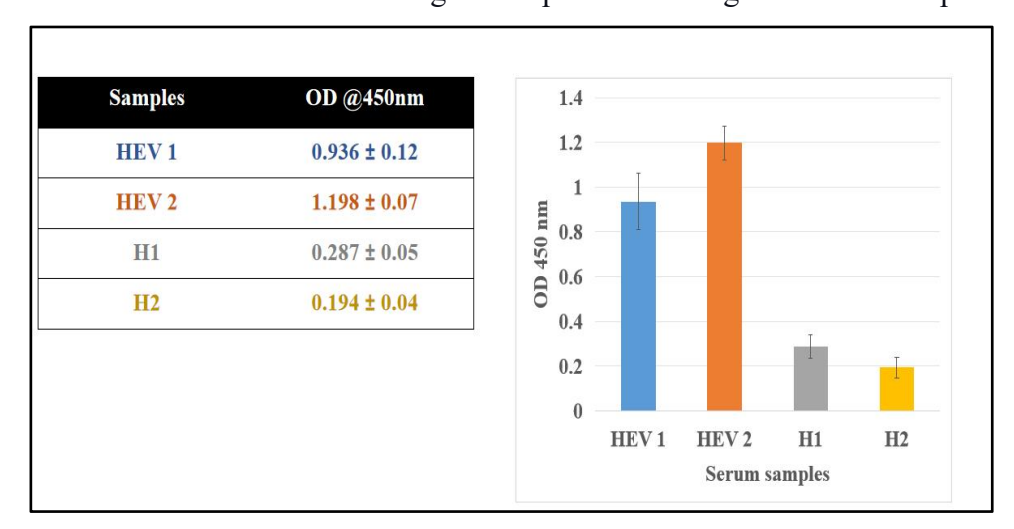


Figure 4.5.1. ELISA graph showing the O.D. at 450 nm of HEV-infected and healthy sera. The graph depicts a significant difference in O.D. of infected patient's sera (higher values) as compared to the healthy one (lower values).

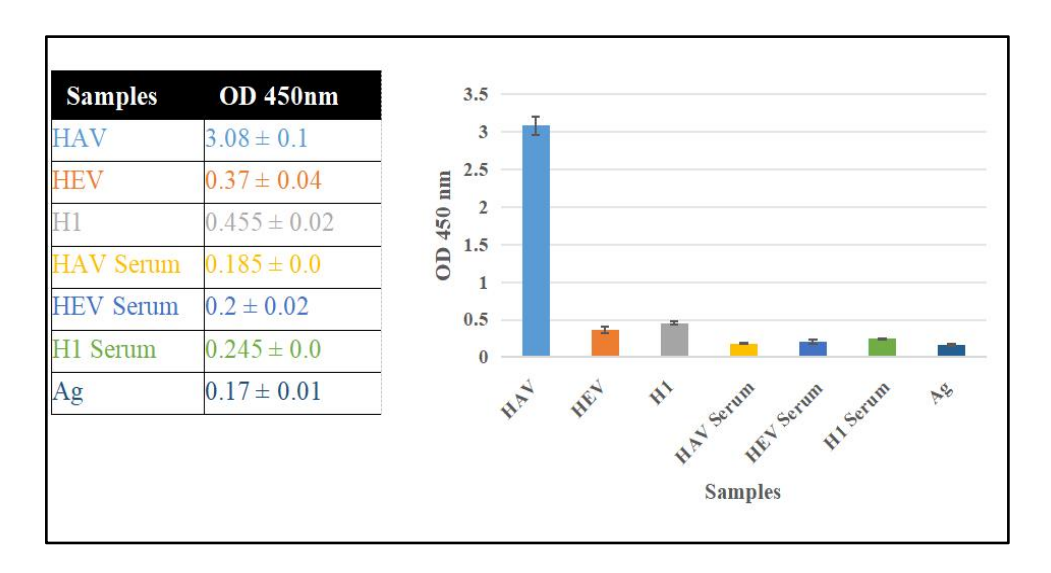


Figure 4.5.2. ELISA graph showing the O.D. at 450 nm of HAV-infected and healthy sera. The graph depicts a significant increase in O.D. of infected patients compared to healthy patients.

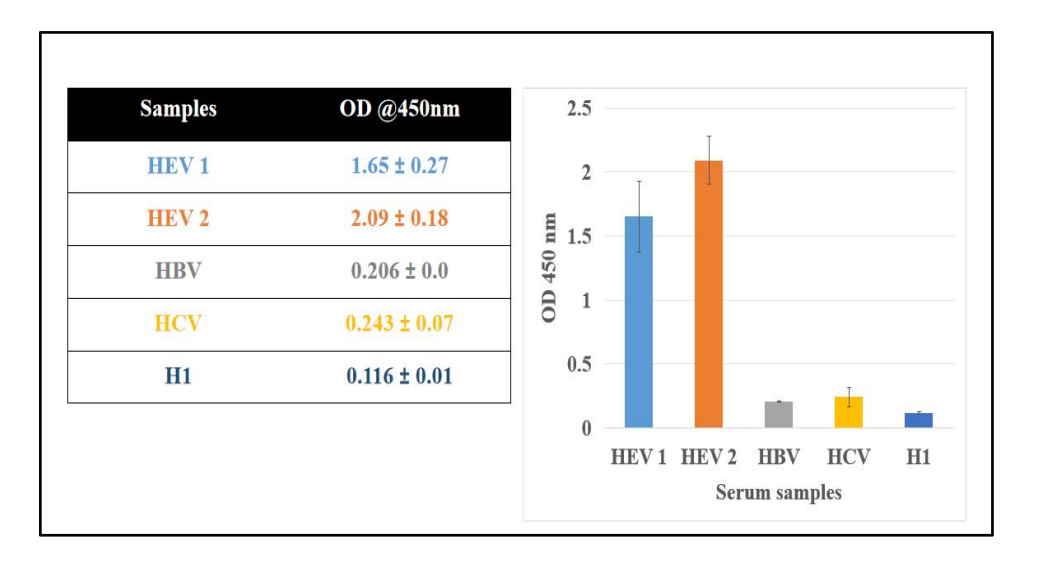


Figure 4.5.3. ELISA graph showing the O.D. at 450 nm of HEV-infected, healthy, HBV and HCV-infected sera. The graph depicts a significant difference in O.D. of HEV-infected patients compared to those in healthy, HBV, and HCV-infected patient sera.

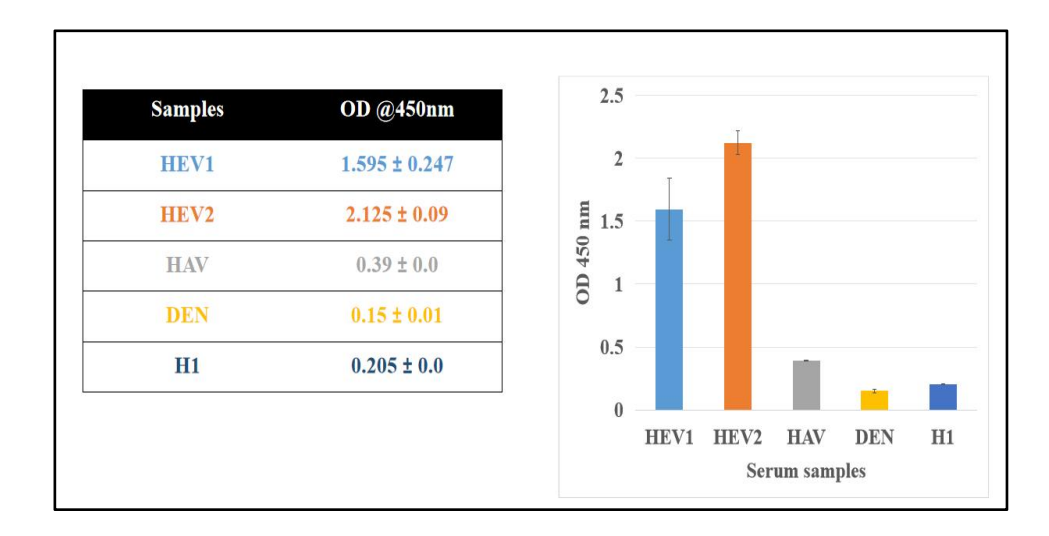


Figure 4.5.4. ELISA graph showing the O.D. at 450 nm of HEV-infected, healthy, HAV and dengue-infected sera. The graph depicts a significant difference in O.D. of HEV-infected patients compared to those with healthy, dengue, and HAV-infected patient sera.

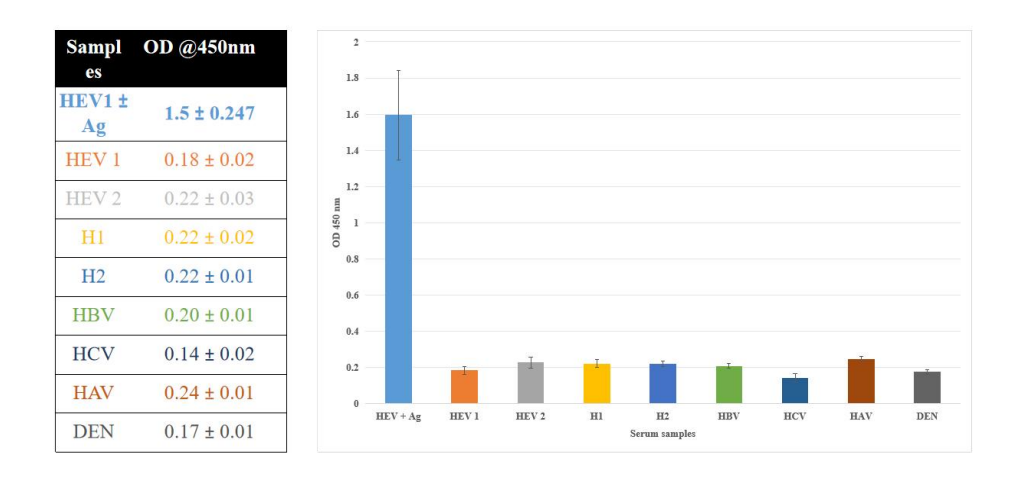


Figure 4.5.5. ELISA graph showing the O.D. at 450 nm of only serum samples without antigen. HEV-infected, healthy, HBV, HCV, HAV, and dengue-infected sera are plotted. The graph shows that the serum without antigen values is much less significant than the abovementioned HEV-positive values.

4.6 Conjugation of AuNPs with protein

Conjugation was performed to develop the kit, as they are responsible for color development after reacting with the antigen on the surface of the nitrocellulose membrane in case of a positive match for the given sample. Conjugation was verified using the spectral analysis performed on a plate reader. Fig. 4.6.1. The spectral graph contains the spectra of pure AuNPs, AuNPs in pH 6.5 buffer, and conjugated AuNPs in pH 6.5 buffer. A max peak of pure AuNPs was observed at 518-520 nm, matching the standard ones. A similar peak was observed in AuNPs dissolved in pH 6.5 buffer. The conjugated AuNPs showed a right peak shift from 518 nm to 530-535 nm. This suggests that conjugation has occurred at a pH of 6.5, around the isoelectric point of the protein (around 5.8), at which the AuNPs are also stable. A stability assay was done by dissolving the pellet obtained after centrifugation of the conjugated AuNPs in the storage buffer. The stability of conjugation was validated by performing spectral analysis. The spectral graph showed a peak at the conjugation maxima, suggesting a stable conjugation (Fig. 4.6.2). The Same method was used for conjugation of HAV Ag2 protein (Fig. 4.6.3).

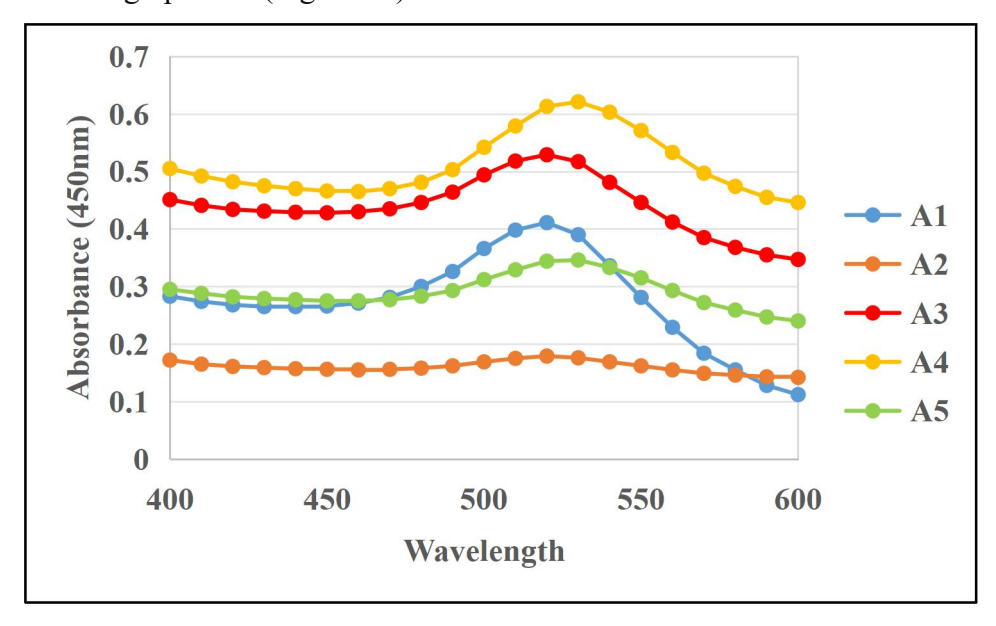


Figure 4.6.1. Spectral graph of conjugated AuNPs, A1 represents AuNPs, A2 represents AuNPs in pH 6.5, A3 represents AuNPs in pH 6.5, A4

represents Conjugated AuNPs in pH 6.5, and A5 represents Conjugated AuNPs in pH 6.5. This shows the conjugation of AuNPs with a shift in the wavelength from 520 nm of AuNPs to 530 nm of conjugated AuNPs.

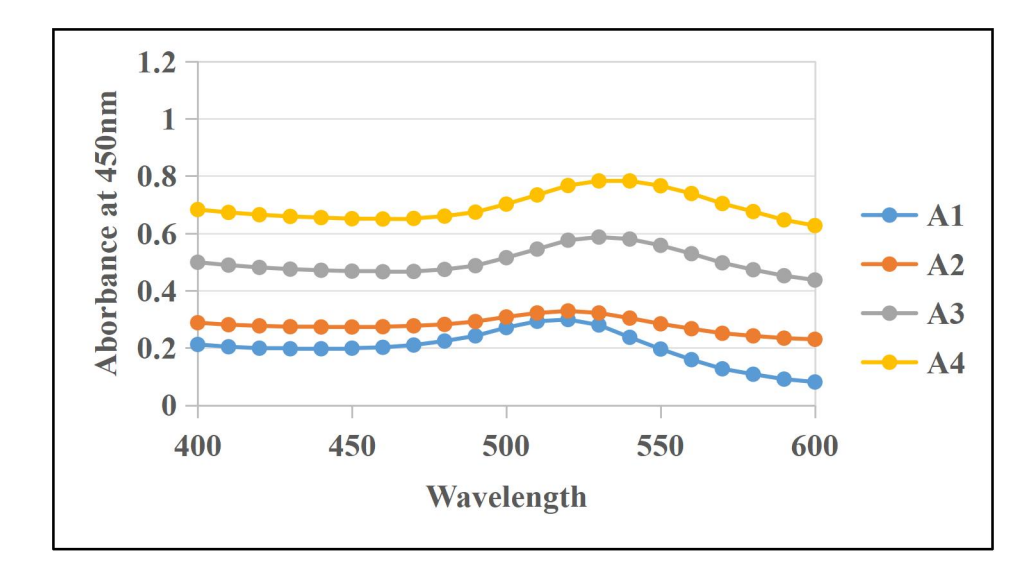


Figure 4.6.2. Spectral graph showing the conjugation of AuNPs in storage buffer, A1 represents AuNPs, A2 represents AuNPs in pH 6.5, A3 represents Conjugated AuNPs in pH 6.5, and A4 represents Conjugated AuNPs in stability buffer. It shows a shift in the wavelength from 520 nm of AuNPs to 530 nm as observed in conjugated AuNPs.

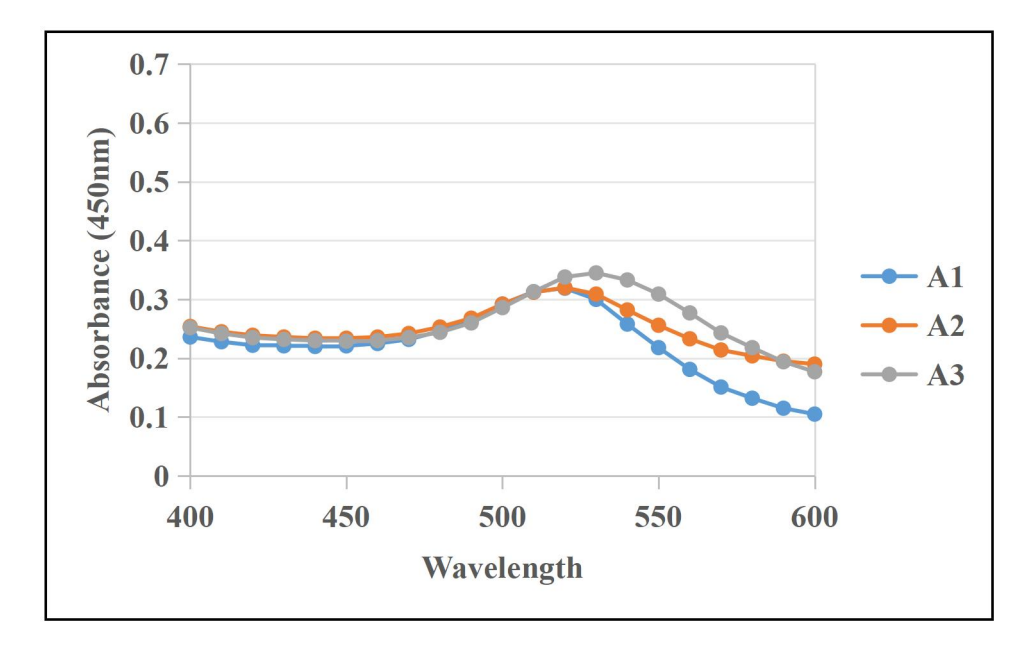


Figure 4.6.3. Spectral graph showing the conjugation of AuNPs with HAV Ag2, A1 represents AuNPs, A2 represents AuNPs in pH 6.5, A3 represents Conjugated AuNPs pH 6.5. It shows a shift in the wavelength from 520 nm of AuNPs to 530 nm as observed in conjugated AuNPs.

4.7 Synthesis of AuNPs

The successful synthesis of gold nanoparticles was carried out using the Turkweich method. A color change was observed when the right amount of citrate was added to the heated gold solution. Intial color was pale yellow that instantly changed to black with almost changing instantly again to wine red indicating formation of gold nanoparticles (Fig. 4.7.1). During the spectral analysis, a peak was observed around 530 nm as depicted in Fig. 4.7.2. For comparison, the synthesized AuNPs were compared with commercial and conjugated with HAV Ag2 protein as well. After conjugation, a shift in peak was observed from 530 to 540 nm, confirming the conjugation of HAV Ag2 protein with the AuNPs (Fig. 4.7.2).

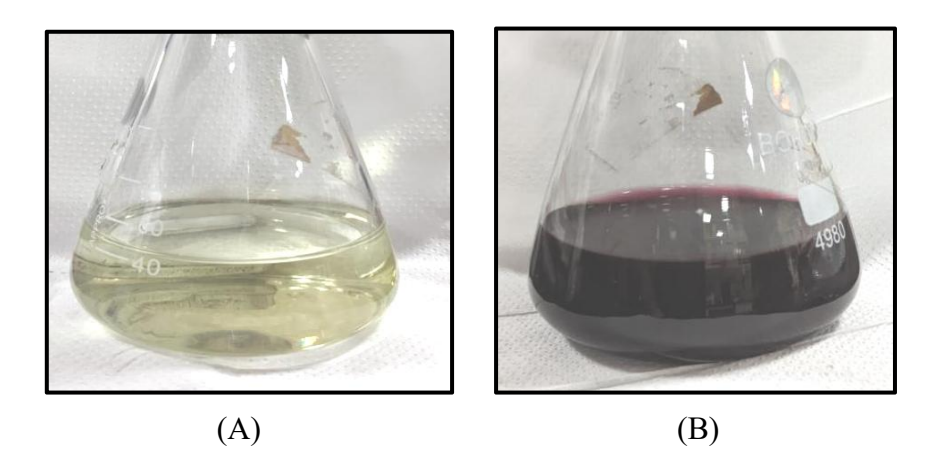


Figure 4.7.1. Synthesis of AuNPs. (A) Distilled water and gold chloride solution appear yellow. (B) Gold nanoparticle formation after adding sodium citrate is observed by changing the color to red.

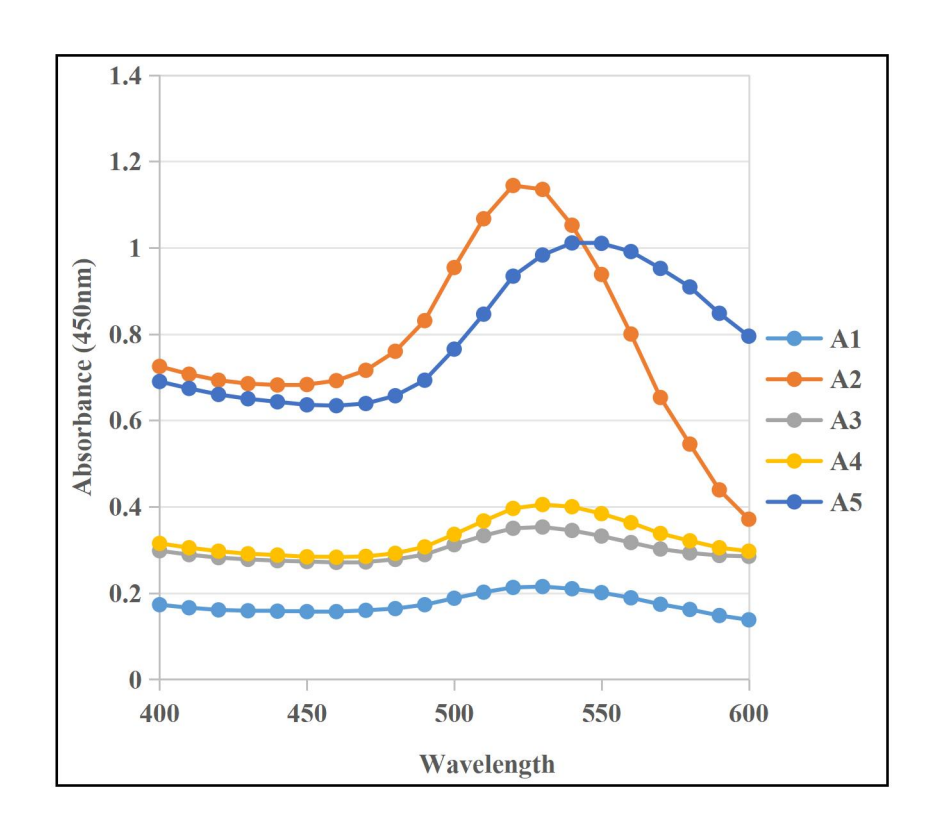


Figure 4.7.2. Spectral graph showing the conjugation of AuNPs with HAV Ag2, A1 represents commercial AuNPs, A2 represents in-house AuNPs, A3 represents in-house AuNPs (concentrated 10 fold), A4 represents conjugated in-house AuNPs with HAV Ag2, A5 represents conjugated in-house AuNPs with HAV Ag2 (concentrated 10 fold). It shows a shift in the wavelength from 530 nm of AuNPs to 540 nm as observed in conjugated AuNPs.

High O.D. gold nanoparticles were synthesized by changing the molar ratio of gold nanoparticles to sodium citrate. Spectral analysis revealed a peak around 530 nm and O.D. of around 2.5 when diluted 4 times and around 1.5 when diluted 8 times (Fig. 4.7.3), resulting in an average O.D. of 11. Further, the synthesized AuNPs were conjugated with HAV Ag2 protein and a shift in peak was observed from 530 nm to 540 nm, confirming the conjugation (Fig. 4.7.4).

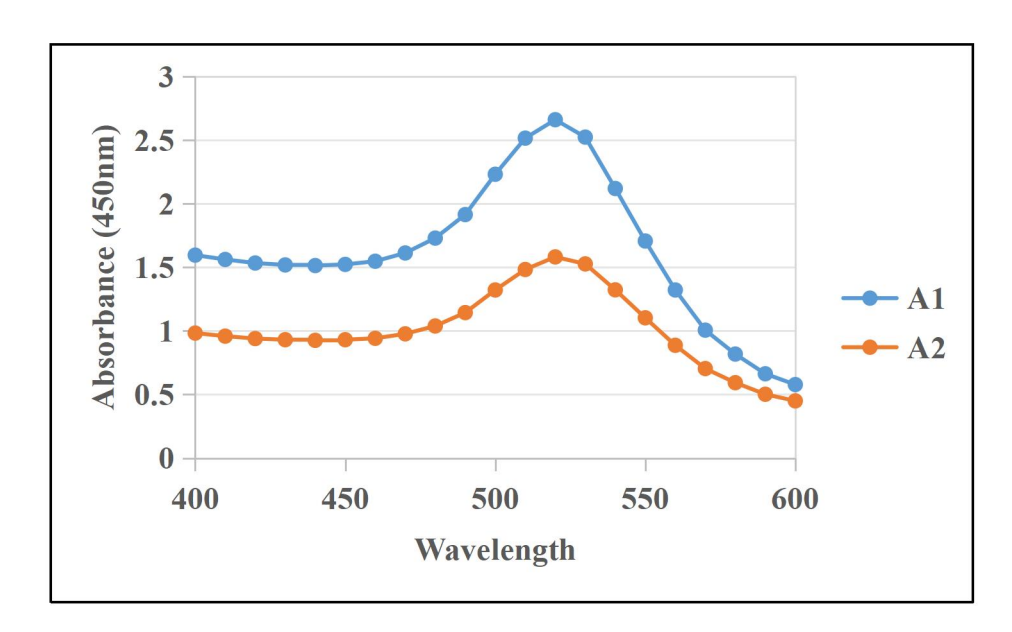


Figure 4.7.3. Spectral graph showing the synthesized high O.D. AuNPs, A1 represents in-house AuNPs diluted 4 times, A2 represents in-house AuNPs diluted 8 times.

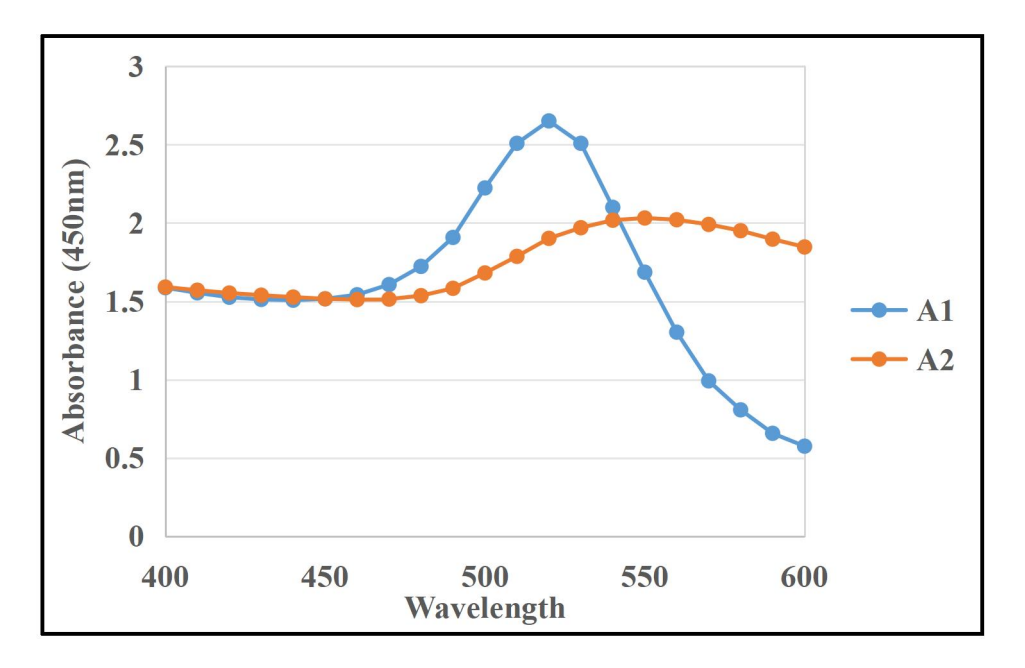


Figure 4.7.4. Spectral graph showing the synthesized high O.D. AuNPs, A1 represents in-house AuNPs diluted 4 times, A2 represents in-house AuNPs conjugated with HAV Ag2. A shift from 530 nm to 540 nm confirms conjugation.

4.8 SEM of synthesized AuNPs

SEM analysis was done to confirm the exact shape and size of the synthesized nanoparticles. The SEM images were analyzed and found to show that the particles were below 100 nm in diameter. They were in a range of 20-50 based on the images obtained through SEM (Fig. 4.8.1). They were also all spherical (Fig. 4.8.1), which was ideal for conjugation.

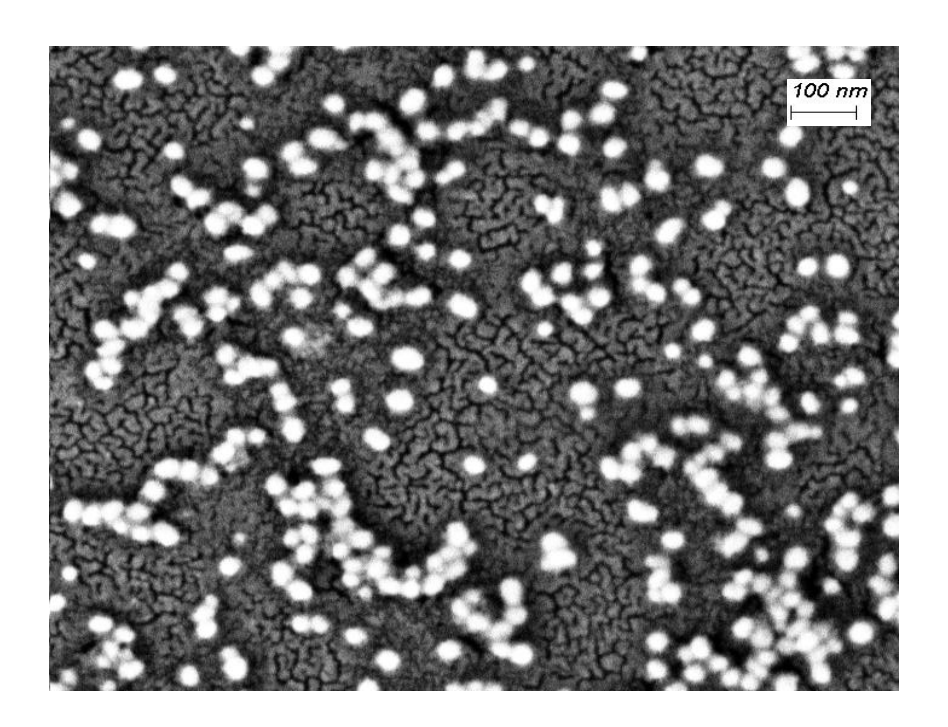


Figure 4.8.1. SEM analysis of synthesized AuNPs. The analysis revealed the size to be in the range of 20-30 nm.

4.9 Optimization of conjugation

The optimization ratios were used to perform the studies, and the spectral analysis was done after plotting the graphs. The uncojugated AuNPs showed a peak max at around 520 nm with an O.D. of around 2.2. All ratios of the conjugated AuNPs showed a shift in the peak maxima from 520 nm to 530 nm, but the O.D. values were slightly different. The O.D. for the 1:10 ratio had decreased less compared to the other. It was still around 2.1. For the 2:10 ratio, the O.D. dropped to 2, which was still

acceptable. However, for a 3:10 ratio of antigen to AuNPs, the O.D. dropped down to almost 1.7 (Fig. 4.9.1). The optimal conjugation was determined after DLS and aggregation studies.

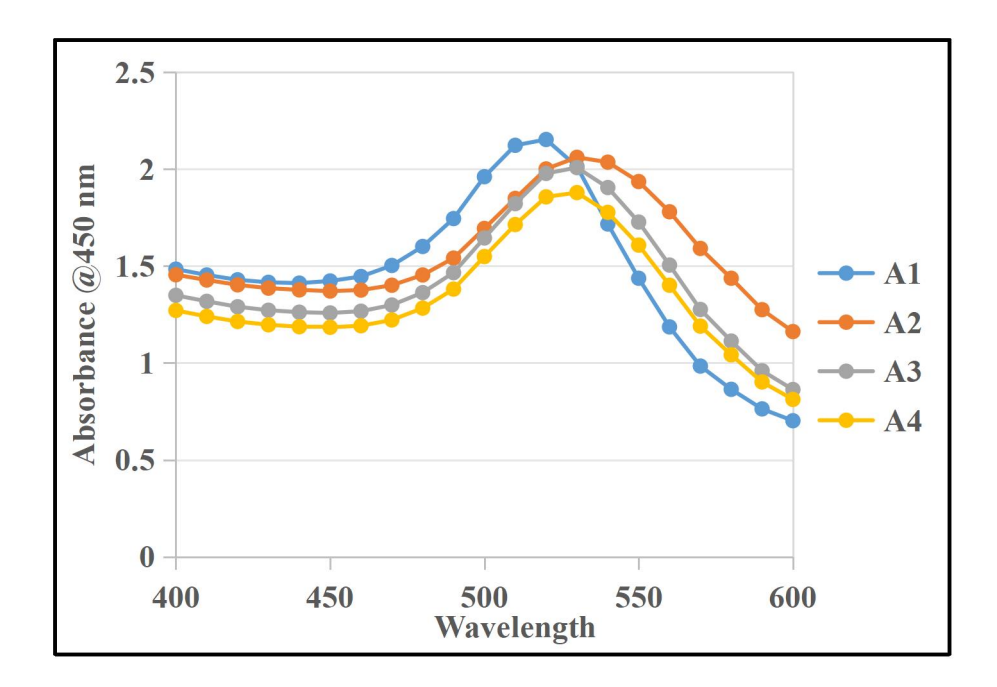


Figure 4.9.1. Spectral graph showing the synthesized high O.D. AuNPs conjugation optimization. A1 represents inhouse unconjugated AuNPs, A2 represents inhouse AuNPs conjugated with HEV Ag1 antigen in the ratio 1:10, A3 represents inhouse AuNPs conjugated with HEV Ag1 antigen in the ratio 2:10, A4 represents inhouse AuNPs conjugated with HEV Ag1 antigen in the ratio 3:10. A shift from 530 nm to 540 nm in A2, 3, 4 confirms conjugation.

4.10 Aggregation studies using a blocking agent

Aggregation studies were done using a blocking agent to check whether the blocking agent successfully prevents aggregation between gold nanoparticles and the antigen. The control MCT showed precipitation in the solution, suggesting aggregation without a blocking agent. However, the blocking agent added gold nanoparticles showed a clear solution, indicating that aggregation had been prevented between the AuNPs and the antigen, as depicted in Fig. 4.10.1. The flow was also tested later, where a

significantly better flow was observed compared to the one with no blocking agent.

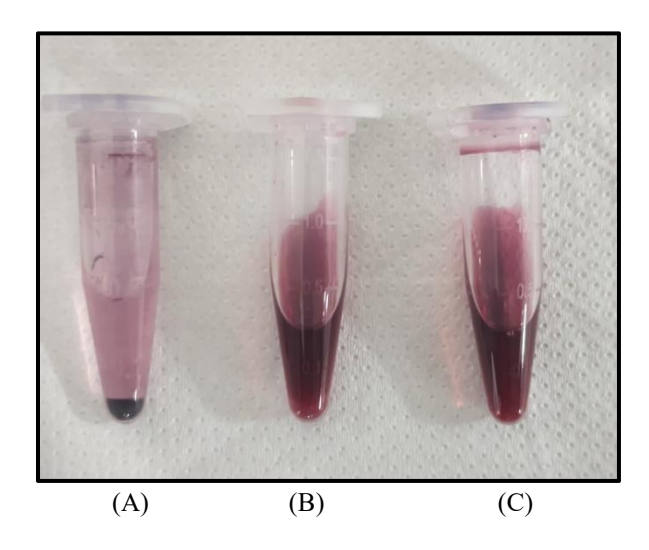


Figure 4.10.1. Aggregation studies using a blocking agent. (A) Antigen plus AuNPs, precipitation was observed, suggesting aggregation in the solution. (B) AuNPs plus a blocking agent showed no change, (C) AuNPs plus antigen plus a blocking agent also showed a clear solution and suggested no aggregation.

4.11 Dipstick assembly results

A dipstick assay was performed to observe the development pattern of the reaction between the antigen and the antibody. The preliminary tests for the dipstick assay resulted in no significant results due to the improper flow of conjugated AuNPs. The early flaw of precipitation would result in the aggregation of conjugated AuNPs at the point of contact and not at the antigen-loaded site. A blocking agent treated AuNPs, however, did not form such lines and due to their high O.D., travelled through the NC membrane in just a few minutes (Fig. 4.11.1). The conjugated AuNPs were able to cover the whole membrane and hence were optimal for testing with serum samples. The conjugated AuNPs treated with HEV-infected serum showed a plain red front at 40 μ L of the serum sample. However, at 80 and 120 μ L of serum samples, a blank spot appeared at the site where the antigen was loaded (antigen concentration- 14 μ g) (Fig. 4.11.2). We tested

the same volumes of serum for healthy patient sera samples. We found no blank spot in the case of infected for healthy serum at any antigen concentration and serum volumes (Fig. 4.11.3).

This indicated that the spot formation was due to some hindrance between the binding of the conjugated antibody with the antigen at the site.

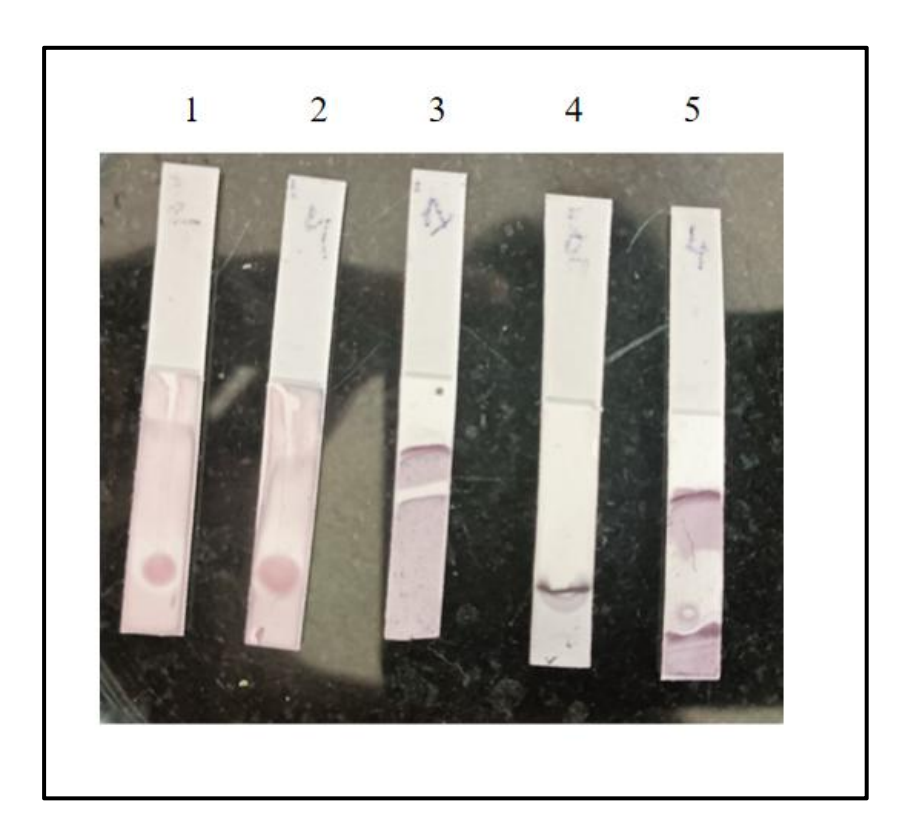


Figure 4.11.1. Dipstick assay with a blocking agent and without a blocking agent, conjugated antigen. (1) a blocking agent conjugated antigen with 14 μ g of antigen on NC, (2) a blocking agent conjugated antigen with 28 μ g of antigen on NC, (3) Without a blocking agent conjugated antigen with 7 μ g of antigen on NC, (4) Without a blocking agent conjugated antigen with 14 μ g of antigen on NC, (5) Without a blocking agent conjugated antigen with 28 μ g of antigen on NC.

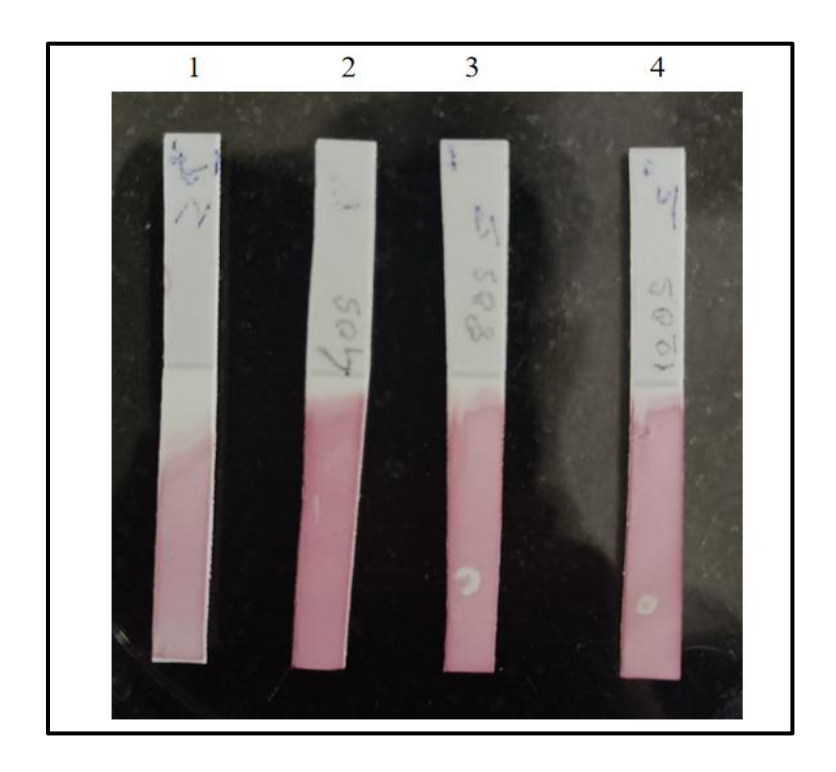


Figure 4.11.2. Dipstick assay with a blocking agent, conjugated antigen, and HEV-infected sera. (1) A blocking agent conjugated antigen with 14 μg of antigen on NC, (2) a blocking agent conjugated antigen with 14 μg of antigen on NC and 40 μL of HEV infected serum, (3) a blocking agent conjugated antigen with 14 μg of antigen on NC and 80 μL of HEV infected serum-blank spot was observed at the site of antigen loading, (4) a blocking agent conjugated antigen with 14 μg of antigen on NC and 120 μL of HEV infected serum-blank spot was observed at the site of antigen loading.

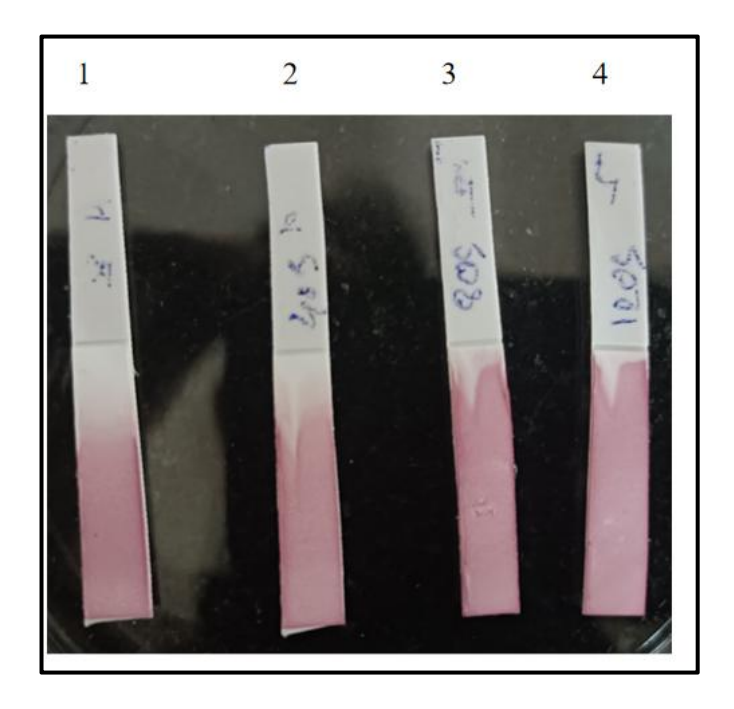


Figure 4.11.3. Dipstick assay with a blocking agent, conjugated antigen, and healthy sera. (1) a blocking agent conjugated antigen with 14 μg of antigen on NC, (2) a blocking agent conjugated antigen with 14 μg of antigen on NC and 40 μL of healthy serum, (3) a blocking agent conjugated antigen with 14 μg of antigen on NC and 80 μL of healthy serum- no blank spot was observed at the site of antigen loading, (4) a blocking agent conjugated antigen with 14 μg of antigen on NC and 120 μL of healthy serum- no blank spot was observed at the site of antigen loading.

4.12 Lateral immunoflow Kit development and assembly

Based on the dipstick assay results, the kit development proceeded. By adding about 200 μ L of infected serum, the flow in the kit was achieved. After 10 minutes, the kit was observed for any valid line formation. Even though significant lines were not observed in any kit, there was some formation of blank spots and solid lines in the kit with conjugated AuNPs of O.D. 10. No such lines were observed in the kit with conjugated AuNPs of O.D. 1. This was a basis of proof that some reaction was happening. With further optimization, the desired results could be obtained.

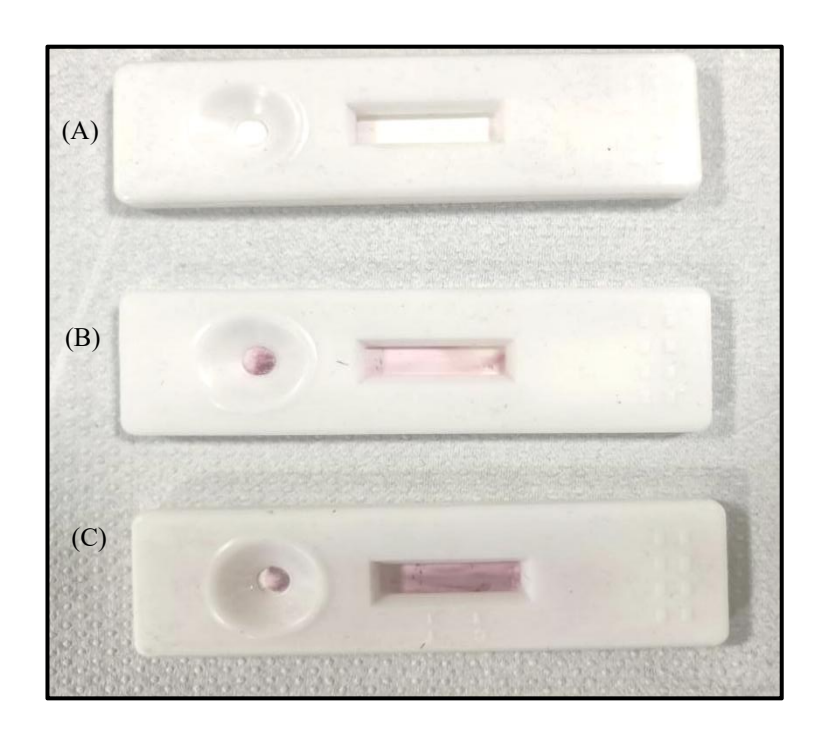


Figure 4.12.1. Development of LFIA kit. (A) Standard kit with no serum, (B) 200 μ L of infected sera and O.D. conjugated AuNPs, no spots or lines were detected, (C) 200 μ L of infected sera and O.D. conjugated AuNPs, mild spots at the C line and lines at the T line were detected.

Chapter 5

Conclusion and Future Directions

The gene for HEV was cloned and expressed in pET43a. We observed that the whole Ag1 region cannot be described using the generated construct. Hence, we used a truncated region to clone and express the data. The expressed protein was solubilized in the urea solution. It was earlier solubilized in N-lauryl sarcosine, but the protein's antigenicity decreased significantly. Hence, we opted for urea. The ELISA results for urea were first tested with different parameters to optimize them. BSA was first used for blocking, and then the course was redirected toward skim milk. Other blocking agents can also be used to reduce the noise-to-signal ratio. Serum concentrations can also be changed using different dilutions and standard diluents. We used BSA as a standard diluent as it was less antigenic towards the antibodies. Different serum samples from those tested here can be analyzed to define the crossreactivity further.

For hepatitis A, as mentioned earlier in the introduction, we chose Ag2 and tried to express it, as earlier work has been done on it. Other immunodominant capsid-forming proteins could be expressed in *E. coli* and used as an antigen in the kit. As for HEV, even HAV Ag2 could be cloned in pET28b and expressed in Rosetta cells. However, we faced the problem of needing more protein yield from the Rosetta strain. Hence, using BL21 (DE3) is recommended, and other expression vectors could also be given a chance. The pellet was resuspended in urea, but other solubilizing agents, such as N-lauryl sarcosine, can also be used. The purified protein of HAV was first precipitated using 1 M ammonium sulfate, but the protein failed to precipitate. Hence, the ammonium sulfate concentration was raised to 2 M, and the protein was later dialyzed. The same ELISA protocol as HEV was followed for HAV.

Conjugation was the most crucial step in the kit development process as it determines the band intensity and overall functionality. The stability of AuNPs is essential for conjugation, and they were tested at different pH ranges. Conjugation of both proteins was successful at this pH. Spectral analysis of the conjugated AuNPs suggested the peak shift from 520 nm to 530 nm, confirming conjugation.

High O.D. AuNP synthesis was necessary to increase the intensity of the line developed on the kit. The synthesized AuNPs showed a higher O.D. at a specific molar ratio of sodium citrate and gold nanoparticles. AuNPs were diluted to perform spectral analysis, as the instrument could not read that much absorbance. Conjugation with the same AuNPs was successful, and the same shift was observed.

A new approach had to be implemented as the dipstick assay results were inadequate. The precipitation problem was hindering the output and needed to be addressed immediately. Precipitation due to aggregation between the gold nanoparticles and both antigens did not allow for the smooth flow of the solution due to capillary action during the dipstick assay and kit development. The particles would aggregate at the point of contact, leading to aggregation at the same site and generating a color line at the spot. This would cause serious false-positive results. To avoid this, we took the help of a blocking agent. Studies have already shown the use of a blocking agent to block the excess charges on the surface of the gold nanoparticles, thereby aiding in conjugation with the respective antigen. A blocking agent was also observed not to hinder the conjugation process when mixed. However, there was no data on whether it affected the antibodies present in the serum during dipstick and kit studies. Another approach was done in parallel to this study, whose data is not included due to insufficient data, using antibodies as the test line against the Fc region of the anti-HV antibodies from the infected patient sera. It has already been experimented and the basic principle behind it revolves around the fact that

the antigen conjugated to the AuNPs will first bind to the anti-HV antibodies from the serum on the conjugate pad and will be captured by the capture antibody (like anti-human IgM) later on the test line will leading to color formation at the site. In contrast, healthy serum will give a precise flow. This method is thought to work as it requires less O.D. of AuNPs (around 1) while giving highly specific and sensitive results.

Appendix-A

Primers used:

Primer	Used as
HEV916F	Forward primer for HEV Ag1
HEV917R	Reverse primer for HEV Ag1
PK998F	Forward primer for HAV Ag2
PK999R	Reverse primer for HAV Ag2

References

- [1] "What is hepatitis?". WHO. July 2016. Archived from the original on 7 November 2016. Retrieved 10 November 2016.
- [2] "Hepatitis". NIAID. Archived from the original on 4 November 2016. etrieved 2 November 2016.
- [3] "Hepatitis". MedlinePlus. Archived from the original on 11 November 2016. Retrieved 10 November 2016.
- [4] "Hepatitis (Hepatitis A, B, and C) | ACG Patients". patients.gi.org. Archived from the original on 2017-02-23.
- [5] Hepatitis World Health Organization (WHO).
- [6] Dienstag, JL (2015). "Chapter 360: Acute Viral Hepatitis". In Kasper, D; Fauci, A; Hauser, S; Longo, D; Jameson, J; Loscalzo, J (eds.). Harrison's Principles of Internal Medicine, 19e. New York, NY: McGraw-Hill. ISBN 978-0-07-180215-4.
- [7] "Hepatitis A Questions and Answers for the Public | Division of Viral Hepatitis | CDC". www.cdc.gov. Archived from the original on 2016-03-12. Retrieved 2016-03-14.
- [8] "Hepatitis E". World Health Organization. Archived from the original on 2016-03-12. Retrieved 2016-03-14.
- [9] Hepatitis B Foundation.
- [10] Hepatitis C- NHS.

- [11] Mayoclinic- Hepatitis C, mayoclinic.org/diseases-conditions/hepatitis-c/diagnosis-treatment/
- [12] Diane Sievert, The Different Types of Hepatitis, July 28, 2023.
- [13] ICTV. "Virus Taxonomy: 2014 Release". Archived from the original on 10 July 2015. Retrieved 15 June 2015.
- [14] Cristina J, Costa-Mattioli M (August 2007). "Genetic variability and molecular evolution of hepatitis A virus". Virus Res. 127 (2): 151–7. doi:10.1016/j.virusres.2007.01.005.
- [15] "Viral Zone". ExPASy. Archived from the original on 17 June 2015. Retrieved 15 June 2015.
- [16] Stapleton JT (1995). "Host immune response to hepatitis A virus". J. Infect. Dis. 171 (Suppl 1): S9–14. doi:10.1093/infdis/171.Supplement_1.S9.
- [17] Stuart DI, Ren J, Wang X, Rao Z, Fry EE. Hepatitis A virus capsid structure. Cold Spring Harb Perspect Med. 2019;9(5):a031807.
- [18] Haro I, Perez JA, Reig F, Pinto RM, Gonzalez-Dankaart JF, Bosch A. Antihepatitis A virus antibody response elicited in mice by different forms of a synthetic Ag2 peptide. Microbiol Immunol. 1995;39(7):485–90.
- [19] Pérez-Gracia MT, Suay-García B, Mateos-Lindemann ML (20 March 2017). "Hepatitis E and pregnancy: current state". Reviews in Medical Virology. 27 (3): e1929. doi:10.1002/rmv.1929.

- [20] Feldman M, Friedman LS, Brandt LJ (2010). Sleisenger and Fordtran's Gastrointestinal and Liver Disease E-Book: Pathophysiology, Diagnosis, Management, Expert Consult Premium Edition Enhanced Online Features. Elsevier Health Sciences. p. 1337. Retrieved 27 June 2020.
- [21] Balakrishnan V, Rajesh G (2016). Practical Gastroenterology. JP Medical Ltd. p. 195. Retrieved 22 July 2019.
- [22] Cocquerel L, Dubuisson J, Meuleman P, d'Autume Vd, Farhat R, Aliouat-Denis CM, Duvet S, Saas L, Wychowski C, Saliou JM, Sayed IM, Montpellier C, Ankavay M (18 April 2019). "New insights into the Ag1 capsid protein, a key player of the hepatitis E virus lifecycle". Scientific Reports. 9 (1): 6243. Bibcode:2019NatSR...9.6243A. doi:10.1038/s41598-019-42737-2.
- [23] Ahmad I, Holla RP, Jameel S (October 2011). "Molecular Virology of Hepatitis E Virus". Virus Research. 161 (1): 47–58. doi:10.1016/j.virusres.2011.02.011.
- [24] Kamar N, Dalton HR, Abravanel F, Izopet J (2014). "Hepatitis E Virus Infection". Clinical Microbiology Reviews. 27 (1): 116–138. doi:10.1128/CMR.00057-13.
- [25] Aggarwal R (2 October 2012). "Diagnosis of hepatitis E". Nature Reviews Gastroenterology & Hepatology. 10 (1): 24–33. doi:10.1038/nrgastro.2012.187.
- [26] Tam AW, Smith MM, Guerra ME, Huang C-C, Bradley DW, Fry KE et al. Hepatitis E virus (HEV): Molecular cloning and sequencing of the full-

- length viral genome. Virology. 1991;185(1):120-31. doi:https://doi.org/10.1016/0042-6822(91)90760-9.
- [27] Hornbeck P, Enzyme-linked immunosorbent assays. Curr Protoc Immunol 2001, doi.org/10.1002/0471142735.im0201s01.
- [28] Engvall E. The ELISA enzyme-linked immunosorbent assay. Clin Chem 2010;56:319–20. doi: 10.1373/clinchem.2009.127803
- [29] Suleyman Aydin, A short history, principles, and types of ELISA, and our laboratory experience with peptide/protein analyses using ELISA, Peptides, Volume 72, 2015, Pages 4-15, ISSN 0196-9781, https://doi.org/10.1016/j.peptides.2015.04.012.
- [30] Park J.H., Park E.K., Cho Y.K., et al. Normalizing the optical signal enables robust assays with lateral flow biosensors. Acs Omega. 2022;7(21):17723–17731. doi: 10.1021/acsomega.2c00793.
- [31] Ali Z., Sanchez E., Tehseen M., et al. Bio-SCAN: a CRISPR/dCas9-based lateral flow assay for rapid, specific, and sensitive detection of SARS-CoV-2. ACS Synth. Biol. 2022;11(1):406–419. doi: 10.1021/acssynbio.1c00499.
- [32] Shyu R.H., Shyu H.F., Liu H.W., et al. Colloidal gold-based immunochromatographic assay for detection of ricin. Toxicon. 2002;40(3):255–258. doi: 10.1016/s0041-0101(01)00193-3.
- [33] Nielsen K., Yu W.L., Kelly L., et al. Validation and field assessment of a rapid lateral flow assay for detection of bovine antibody to Anaplasma marginale. J. Immunoass. Immunochem. 2009;30(3):313–321. doi: 10.1080/15321810903084749.

- [34] Morales-Narvaez E., Naghdi T., Zor E., et al. Photoluminescent lateral-flow immunoassay revealed by graphene oxide: highly sensitive paper-based pathogen detection. Anal. Chem. 2015;87(16):8573–8577. doi: 10.1021/acs.analchem.5b02383.
- [35] Mei Z., Qu W., Deng Y., et al. One-step signal amplified lateral flow strip biosensor for ultrasensitive and on-site detection of bisphenol A (BPA) in aqueous samples. Biosens. Bioelectron. 2013;49:457–461. doi: 10.1016/j.bios.2013.06.006.
- [36] Ngom B., Guo Y., Wang X., et al. Development and application of lateral flow test strip technology for detection of infectious agents and chemical contaminants: a review. Anal. Bioanal. Chem. 2010;397(3):1113–1135. doi: 10.1007/s00216-010-3661-4.
- [37] Kuang H., Xing C., Hao C., et al. Rapid and highly sensitive detection of lead ions in drinking water based on a strip immunosensor. Sensors (Basel) 2013;13(4):4214–4224. doi:10.3390/s130404214.
- [38] Alhabbab R.Y. Lateral flow immunoassays for detecting viral infectious antigens and antibodies. Micromachines (Basel). 2022;13(11):1901. doi: 10.3390/mi13111901.
- [39] Moshe M., Daunt A., Flower B., et al. SARS-CoV-2 lateral flow assays for possible use in national covid-19 seroprevalence surveys (react 2): diagnostic accuracy study. Bmj. 2021;372 doi: 10.1136/bmj.n423.
- [40] Plotz C.M., Singer J.M. The latex fixation test. I. Application to the serologic diagnosis of rheumatoid arthritis. Am. J. Med. 1956;21(6):888–892. doi: 10.1016/0002-9343(56)90103-6.

- [41] Boehringer H.R., O'Farrell B.J. Lateral flow assays in infectious disease diagnosis. Clin. Chem. 2021;68(1):52–58. doi: 10.1093/clinchem/hvab194.
- [42] Wang Y., He Z., Ablimit P., et al. Development of multiplex cross displacement amplification combined with lateral flow biosensor assay for detection of virulent shigella sonnei. Front. Cell. Infect. Microbiol. 2022;12:1012105. doi: 10.3389/fcimb.2022.1012105.
- [43] Bishop J.D., Hsieh H.V., Gasperino D.J., et al. Sensitivity enhancement in lateral flow assays: a systems perspective. Lab Chip. 2019;19(15):2486–2499. doi: 10.1039/c9lc00104b.
- [44] Sapsford KE, Algar WR, Berti L, Gemmill KB, Casey BJ, Oh E, Stewart MH, Medintz IL (March 2013). "Functionalizing nanoparticles with biological molecules: developing chemistries that facilitate nanotechnology". Chemical Reviews. 113 (3): 1904–2074. doi:10.1021/cr300143v.
- [45] Zeng S, Yong KT, Roy I, Dinh XQ, Yu X, Luan F (2011). "A review on functionalized gold nanoparticles for biosensing applications" (PDF). Plasmonics. 6 (3): 491–506. doi:10.1007/s11468-011-9228-1.
- [46] Yang X, Yang M, Pang B, Vara M, Xia Y (October 2015). "Gold Nanomaterials at Work in Biomedicine". Chemical Reviews. 115 (19): 10410–88. doi:10.1021/acs.chemrev.5b00193.
- [47] Chiodo F, Marradi M, Tefsen B, Snippe H, van Die I, Penadés S (2013). "High sensitive detection of carbohydrate binding proteins in an ELISA-solid phase assay based on multivalent glyconanoparticles". doi:10.1371/journal.pone.0073027.

[48] Makhsin SR, Razak KA, Noordin R, Zakaria ND, Chun TS. The effects of size and synthesis methods of gold nanoparticle-conjugated MαHIgG4 for use in an immunochromatographic strip test to detect brugian filariasis. Nanotechnology. 2012 Dec 14;23(49):495719. doi: 10.1088/0957-4484/23/49/495719.